Organized Nanostructures of Thermoresponsive Poly(N-isopropylacrylamide) Block Copolymers Obtained Through Controlled RAFT Polymerization

Markus Nuopponen

Laboratory of Polymer Chemistry
Department of Chemistry
University of Helsinki
Finland

ACADEMIC DISSERTATION
FOR THE DEGREE OF DOCTOR OF PHILOSOPHY

To be presented with the permission of the Faculty of Science of the University of Helsinki for public criticism in Auditorium A110 of the Department of Chemistry, on May 9th, 2008, at 12 o'clock.

Helsinki 2008

Opponent

Professor Eva Malmström
Kungliga Tekniska Högskolan
Sweden

Reviewers

Professor Françoise Winnik
Department of Chemistry and Faculty of Pharmacy
University of Montreal
Canada

&

Professor Jukka Seppälä
Laboratory of Polymer Technology
Helsinki University of Technology
Finland

ISBN 978-952-92-3707-4 (paperback)
ISBN 978-952-10-4638-4 (pdf)
http://ethesis.helsinki.fi
Yliopistopaino
Helsinki 2008

Preface

This work was carried out at the Laboratory of Polymer Chemisty, University of Helsinki during the years 2001-2007 under supervision of Professor Heikki Tenhu.
I express my greatest thanks to him for all of the encouragement and supervision.

I thank all the people I have collaborated during these years. I am grateful to the co-authors, especially Dr. Vladimir Aseyev for the help with the light scattering measurements, Dr. Sami Hietala for the NMR measurents, Dr. Jun Shan for fruitful work with gold nanoparticles, Katriina Kalliomäki, Jussi Ojala and Dr. Antti Laukkanen for the help with polymer syntheses. Academy Professor Olli Ikkala, Professor Janne Ruokolainen and Antti Nykänen in Helsinki University of Technology are appreciated for the inspiring teamwork. Professor Françoise Winnik and Professor Jukka Seppälä are acknowledged for the revisions and suggestions that helped me to improve my thesis.

The former and present members of the Laboratory of Polymer Chemistry deserve my thanks for making the laboratory a nice working environment.

I am grateful to the Oskar Öflund Foundation, Tekniikan Edistämissäätiö, Orion-Farmos Foundation and Chancellor of the University of Helsinki for grants. The research was funded by the Finnish Funding Agency for Technology and Innovation and ESPOM graduate school.

Finally, I thank my family for all the support, endless love, encouragement and belief in me over the years. And Susanna, thank you for your unfailing understanding and support.

Helsinki, February 2008

Markus Nuopponen

Abstract

New controlled radical polymerization methods, including reversible addition fragmentation chain transfer (RAFT) polymerization, allow the synthesis of a variety of novel polymer architectures having exciting structure-property-function relations. In this work, well defined amphiphilic block copolymers of thermoresponsive *N*-isopropylacrylamide) (NIPAM) have been successfully synthesized by RAFT polymerization. It is demonstrated, how different pre-designed and precisely synthesized block copolymer materials organize and form specific structures on the nanoscale, mainly in aqueous solutions.

RAFT polymerization was used to build up diblock copolymers comprising of a hydrophilic PNIPAM block and a hydrophobic block, either polystyrene (PS) or poly(*tert*-butylmethacrylate). Polymers were transferred to water, where crew-cut particles or large aggregates were obtained depending on the relative lengths of blocks. Light scattering and microcalorimetry studies were performed on aqueous solutions to investigate the phase transition behavior of aggregates. Large aggregates collapse upon heating whereas crew-cut particles are stabilized in a way what hinders the compression of PNIPAM chains.

A series of poly(styrene-*block*-N-isopropylacrylamide-*block*-styrene) triblock copolymers was synthesized the where hydrophobic PS end blocks were selected to form the minority component, whereas the PNIPAM middle block was the majority component. The self-assembly of poly(styrene-*block*-N-isopropylacrylamide-*block*-styrene) in bulk was studied using transmission electron microscopy (TEM). Lamellar, cylindrical, spherical, and gyroid morphologies were observed in the bulk state. Hydrogels of triblock copolymers can be used as thermoresponsive membrane materials.

A-B-A stereoblock polymers with atactic PNIPAM as a hydrophilic block (either A or B) and a non water-soluble block consisting of isotactic PNIPAM were synthesized using RAFT polymerization. Yttrium trifluoromethanesulfonate was used in the tacticity control. Stereoblock polymers were dispersed in water to spontaneously form, depending on their chain configuration, micelles with different structures. The structures of the A-B-A stereoblock polymers were characterized using light scattering methods, microcalorimetry and UV-vis spectrophotometry. The self-organization and thermally-induced phase separation of stereoblock polymers is strongly affected by the block sequence, but they are not notably affected by the concentration or thermal history of the polymers.

Aqueous dispersions of gold nanoparticles protected with stimuli-sensitive polymers were studied as a function of pH and temperature. The gold nanoparticles were coated with PNIPAM or with the block copolymer poly(methacrylic acid-*block*-N-isopropylacrylamide), where the NIPAM block is bound to the particle surface and poly(methacrylic acid) form the outer layer. The changes in the absorption maxima of the surface plasmon resonance, SPR, of the gold particles were investigated as a function of pH and temperature.

Abbreviations and symbols

Abbreviations

AIBN	2,2'-Azo-bis-isobutyronitrile
ATRP	Atomic transfer radical polymerization
BDAT	S,S'-bis(α,α'-dimethyl-α"-acetic acid)-trithiocarbonate
CDB	2- phenyl-prop-2-yl dithiobenzoate (cumyl dithiobenzoate)
CPA	4-cyanopentanoic acid dithiobenzoate
CRP	Controlled radical polymerization
CTA	Chain transfer agent
DLS	Dynamic light scattering
DMF	Dimethylformamide
DSC	Differential scanning calorimetry
DT	Degenerative transfer
HRTEM	High-resolution transmission electron microscopy
LCST	Lower critical solution temperature
NMP	Nitroxide mediated polymerization
NMR	Nuclear magnetic resonance
PDI	Polydispersity index
PMAA	Poly(methacrylic acid)
PMAA-PNIPAM	Poly(methacrylic acid-*block*-N-isopropylacrylamide)
PNIPAM	Poly(N-isopropylacrylamide)
PNIPAM-PS	Poly(N-isopropylacrylamide-*block*-polystyrene)
P(*t*-BMA)-PNIPAM	Poly(*tert*-butylmethacrylate-*block*-N-isopropylacrylamide)
PS	Polystyrene
PS-PNIPAM-PS	Poly(styrene-*block*-N-isopropylacrylamide-*block*-styrene)
RAFT	Reversible addition-fragmentation chain transfer
SEC	Size exclusion chromatography
SLS	Static light scattering
SPR	Surface plasmon resonance
t-BMA	*tert*-butylmethacrylate
TGA	Thermogravimetric analysis
THF	Tetrahydrofuran
$Y(OTf)_3$	Yttrium trifluoromethanesulfonate

Symbols

D	Diffusion coefficient
d*n*/d*c*	Refractive index increment
ΔH	Change of enthalpy
M_n	Number average molecular weight
M_w	Weight average molecular weight
M_w/M_n	Polydispersity
<ρ>	density
R_g	Radius of gyration
R_h	Hydrodynamic radius
T_g	Glass transition temperature

List of original papers

This thesis is based on the following six publications, hereafter referred to by their Roman numerals (I-VI). Some unpublished material is also presented.

I. Shan, Jun; Nuopponen, M.; Jiang, H.; Kauppinen, E.; Tenhu, H. **Preparation of Poly(N-isopropylacrylamide)-Monolayer-Protected Gold Clusters: Synthesis Methods, Core Size, and Thickness of Monolayer.** *Macromolecules* **2003**, 36, 4526-4533.

II. Nuopponen, M.; Ojala, J.; Tenhu, H. **Aggregation Behaviour of Well Defined Amphiphilic Diblock Copolymers with Poly(N-isopropylacrylamide) and Hydrophobic Blocks.** *Polymer* **2004**, 45, 3643-3650.

III. Nuopponen, M.; Tenhu, H. **Gold Nanoparticles Protected with pH and Temperature Sensitive Diblock Copolymers.** *Langmuir* **2007**, 23, 5352-5357.

IV. Nykänen, A.; Nuopponen, M.; Laukkanen, A.; Rytelä, M.; Turunen, O.; Mezzenga, R., Tenhu, H.; Ikkala, O.; Ruokolainen, J. **Phase Behavior and Temperature-Responsive Molecular Filters Based on Self-Assembly of Polystyrene-*block*-Poly(*N*-isopropylacrylamide)-*block*-Polystyrene.** *Macromolecules* **2007**, 40, 5827-5834.

V. Nuopponen, M.; Kalliomäki, K.; Laukkanen, A.; Hietala, S.; Tenhu, H. **A – B – A Stereoblock Copolymers of N-isopropylacrylamide.** *J. Polym. Sci., Part A: Polym. Chem.* **2008**, 46, 38-46.

VI. Nuopponen, M.; Kalliomäki, K.; Aseyev, V.; Tenhu, H. **Spontaneous and Thermally Induced Self-organization of A – B – A Stereoblock Copolymers of N-isopropylacrylamide in Aqueous Solutions.** *Macromolecules* **2008**, submitted

Authors's contribution to the publications I and IV:
Markus Nuopponen was in close cooperation with the first authors to draw up the research plan and prepare the manuscript for the publications I and IV. Markus Nuopponen was responsible for the polymer syntheses and characterization. For the rest of the publications, Markus Nuopponen independently drew up the research plan and wrote the manuscripts.

Alongside this thesis, the author has contributed several other publications, which are directly related to this thesis:

Raula, J.; Shan, J.;Nuopponen, M.; Niskanen, A.; Jiang, H.; Kauppinen, E.; Tenhu, H. **Synthesisof Gold Nanoparticles Grafted with a Thermo-Responsive Polymer by Surface-Induced Reversible-Addition-Fragmentation Chain Transfer Polymerization.** *Langmuir* **2003,** 19, 3499-3504.

Shan, J.; Chen, J.; Nuopponen, M.; Tenhu, H. **Two Phase Transitions of Poly(N-isopropylacrylamide) Brushes Bound to Gold Nanoparticles.** *Langmuir* **2004,** 20, 4671-4676.

Shan, J.; Nuopponen, M.; Jiang, H.; Viitala, T.; Kauppinen, E.; Kontturi, K.; Tenhu, H. **Amphiphilic Gold Nanoparticles Grafted with Poly(N-isopropylacrylamide) and Polystyrene.** *Macromolecules* **2005,** 38, 2918-2926.

Aseyev, V.; Hietala, S.; Laukkanen, A.; Nuopponen, M.; Confortini, O.; Du Prez, F.; Tenhu, H. **Mesoglobules of Thermoresponsive Polymers in Dilute Aqueous Solutions Above the LCST.** *Polymer* **2005**, 46, 7118-7131.

Shan, J.; Chen, H.; Nuopponen, M.; Tenhu, H. **Optical Properties of Thermally Responsive Amphiphilic Gold Nanoparticles Protected with Polymers.** *Langmuir* **2006**, 22, 794-801.

Hietala, S.; Nuopponen, M.; Kalliomäki, K.; Tenhu, H. **Thermoassociating Poly(N-isopropylacrylamide) A-B-A Stereoblock Copolymers.** *Macromoleculer* **2008,** 41, 2627-2631.

Nykänen, A.; Nuopponen, M.; Hiekkataipale, P.; Hirvonen, S.; Soininen, A.; Tenhu, H.; Ikkala, O.; Mezzenga, R.; Ruokolainen, J. **Cryo-TEM Study of Polystyrene-block-Poly(N-isopropylacrylamide)-block-Polystyrene Temperature-Responsive Hydrogels** *Macromolecules,* **2008**, accepted.

The author has also presented the results covered in this thesis at several international conferences.

Contents

INTRODUCTION

1.1 Background

Self-organization of molecular building blocks is one of the most promising topic in material science.[1-3] In nanoscience and nanotechnology, the self-assembly[4] of synthetic preformed molecules plays an essential role. The main advantage of such 'bottom-up' approach is that materials can be pre-designed at the molecular level to self-assemble, and form specific structures at the nanoscale. Living cells self-assemble as well, and therefore, it is crucial to understand the concept of self-assembly to understand important structures in biology.[5, 6]

However, the block copolymer self-assembly is still a relatively new topic and designing novel polymer based materials is an essential challenge of polymer science. The requirement for self-assembly is that the building blocks contain moieties able to interact in specific environments; solid state, solution, dispersions etc. The polymeric building block in this review means a macromolecule having functional units, which lead to intermolecular attractions: Hydrophobic and hydrophilic effects, hydrogen bonding and coulombic forces.

The block copolymers, consisting of connected sequences formed by two or more different monomer species, have raised an increasing interest due to their unique self-assembly properties as a consequence of their molecular structure.[7] The block copolymers organize into unprecedented morphologies either in dilute or semidilute solutions or in the solid state. In dilute solutions, block copolymers form fascinating colloidal aggregates such as polymeric nanoparticles, micelles or vesicles.[8-10] Similarly in the bulk, block copolymers made of incompatible segments phase separate into nanophases, forming new structures for material science.[11, 12]

Controlled radical polymerization (CRP) techniques are modern alternatives to the living anionic polymerizations for preparing polymeric building blocks.[13, 14] These methods emerged in the mid-1990s, and since then these techniques have been intensively studied as they combine the simplicity of conventional radical polymerization and the living character of anionic polymerization. This allows the synthesis of a variety of novel polymer architectures having exciting structure-property-function relations, such as block and graft copolymers, stars, brushes and bottle-brush structures from a huge amount of different monomers.[15] These materials were hardly known a decade ago.

Stimuli-responsive polymers are polymers that undergo relatively large, physical or chemical property changes in response to small external stimuli such as changes in temperature, pH, electric field or ionic strength.[16] Such polymers are widely found in living systems, and can take many forms. Recent interest in intelligent polymer systems has focused on aqueous polymer solutions, aqueous-solid interfaces and crosslinked hydrogels. Considering the numerous possibilities in designing stimuli-responsive block copolymer architectures by CRP,[17, 18] an infinite variety of materials can be predicted. Thus, in the last few years, the influence of external stimuli on the solution behavior of micellar structures has been increasingly investigated.

Colloidal nanoparticles and noble metal colloids display fascinating opportunities as a consequence of their dimensions and large surface area.[19] Even if the properties of the nanoparticles are size dependent, the surface of the nanoparticles

determines most of their properties in relation to their environment. The development of nanoparticles bearing well defined capping ligands of various compositions has enable the nanochemistry field to reach previously unseen possibilities.[20] The capping ligand is critical to most of the envisioned applications for nanoparticle materials. Functional polymers have turned out to be good stabilizing agents to protect the nanoparticle from coagulation, providing simultaneously facile surface functionalization.[21]

There has been a growing demand for functionalized, well-defined materials as building blocks in nanotechnology applications.[2, 22, 23] 'Smart' block copolymer materials have an enormous potential for applications in medicine and biotechnology such as components of tissue and bone engineering, diagnostics kits, controlled drug release systems, drug targeting and many others. Technological applications of these block copolymers include cosmetics and dispersants for pigments and for inorganics such as carbon nanotubes and nanoparticles. Dense polymer layers improve lubrication, facilitate surface patterning and prevent corrosion. Other potential solid state applications include nanoelectronics, soft lithography, optoelectorics and membranes.

1.2 Review

1.2.1 Controlled radical polymerization

Control over some of the key elements of macromolecular structures such as molecular weight (M_W), polydispersity, end functionality, chain architecture, and composition is one of the most intensively studied areas in polymer science. Until relatively recently, ionic polymerizations (anionic and cationic) were the only "living" techniques available that efficiently controlled the structure and architecture of vinyl polymers.[24-26]Although these techniques assure low-polydispersity materials and controlled molecular weight, ionic living polymerization requires stringent conditions (including exclusion of water and oxygen, and the use of ultrapure reagents), and are limited to a small number of monomers.[27] Thus, it is desirable to prepare, by free radical polymerization, new well-defined block and graft copolymers, stars, end-functional polymers and many other materials under mild conditions and from a larger range of monomers than available for ionic living polymerization. Radical processes can also be implemented in an emulsion, suspension, solution or in the bulk. These are the primary driving forces for the dramatic increase in interest for academic and industrial research in controlled/"living" radical polymerization.[13]

Conventional radical polymerization is not a living polymerization, because it is subjected to significant termination reactions. This can be altered by reducing the importance of the termination steps. The most successful pathways for reducing the termination step in radical polymerization rely on the chemical equilibrium between low concentration of active growing chains and a large amount of dormant chains, which are unable to propagate or terminate. The most important difference between conventional and CRP is the lifetime of an average chain. In conventional systems, a chain is born, grows and dies within approximately 1s. On the other hand, under controlled conditions, a chain grows during several hours enabling precise macromolecular engineering. Long life time of the chain, as mentioned, requires sufficiently low concentration of macroradicals. One of the primary requirements for a radical is that it undergoes reversible termination of the propagating chain end without being involved in unwanted termination or side reactions. Thus, the concentration of reactive chain ends in extremely low, minimizing irreversible termination reactions, such as combination or

disproportionation. Under such conditions, radical polymerization exhibits a living behavior. However, since terminations cannot be completely suppressed in radical processes, such polymerizations are not called 'living' but controlled radical polymerizations. The rationale for uniform terminology, living or controlled, is thoroughly discussed in science community.[28, 29]

CRP techniques have an enhanced tolerance and greater availability of functional groups compared to ionic polymerization. The initial block can be characterized and stored before proceeding to the second block. This is totally unlike ionic procedures and is extremely useful from a synthetic viewpoint, enabling novel block copolymers to be prepared. Requirements for CRP (fast exchange equilibrium, suppressed termination and quantitative initiation) can be met using various chemical systems, but the three currently most promising CRP techniques are stable free radical polymerization, most commonly nitroxide mediated polymerization (NMP),[30, 31] atom transfer radical polymerization (ATRP) and degenerative chain transfer methods (DT),[32] especially reversible addition-fragmentation chain transfer (RAFT) polymerization.[33]

In NMP, nitroxides are used as persistent radical to trap the growing polymer chains in a reversible manner.[34] Nitroxides are stable free radicals that are generally used in organic chemistry to trap radical species. Nitroxides can control the initiation and termination steps in various polymerizations. This was reported by Solomon et al. already in the mid-1980s, but for commercial reasons data was not open to the scientific literature at that time.[35] The first example of modern CRP was controlled polymerization of styrene in the presence of benzoyl peroxide and a stable nitroxide TEMPO (2,2,6,6,-tetramethyl-1-piperidynyl-N-oxy).[30] Similarly, unimolecular initiators based on alkoxyamines have been developed.[31] Control in NMP is achieved with dynamic equilibration between dormant chains capped by a alkoxyamine moiety and actively propagating radicals. NMP was historically the first CRP technique, but it has lost its popularity over the last few years. The main reasons for this are probably the limited range of monomers that can be controlled by NMP and elevated temperature required for the polymerization to procedure. However, the NMP method should be considered as a useful synthetic tool for preparing styrene derivatives, acrylates, acrylamides.

ATRP was discovered independently by Sawamoto and coworkers[36] and Wang and Matyjaszewski in 1995.[32] Similarly to NMP, ATRP is based on the reversible termination process and is under the control of the persistent radical effect.[37] ATRP is controlled by redox equilibrium between macroradicals and dormant species protected by halogen atoms. The initiation systems for ATRP consist of a transition metal/ligand complex and an initiator, typically an activated organic halide. The most commonly used transition metal catalysts for ATRP are based on either copper or ruthenium.

Today, ATRP is the most used CRP method. The dominance of ATRP is probably due to its experimental simplicity and to the commercial availability of most ATRP initiators and catalysts. However, although ATRP is a powerful method, the removal of metallic ions from polymers is an unresolved issue on the industrial scale. In this respect, the recent industrially relevant development for the production of block copolymers was the realization that the relative concentration of catalyst to initiator could be significantly decreased when the reducing agent is present in excess relative to the catalyst. This activator regenerated by electron transfer (ARGET) ATRP method is used with good control for the acrylate and styrene polymerizations.[38, 39]

Processes based on degenerative transfer (DT) operate under very different principles than NMP or ATRP. CRP based on DT do not obey the persistent radical effect. A steady state concentration is established via initiation and termination processes as in conventional radical polymerization. A small amount of growing radicals undergo degenerative exchange with dormant species via a bimolecular transfer process. When dynamic equilibrium is established, all chains have an equal opportunity to grow through an intermediate that is a state between their active and dormant forms. This idea was first conceptualized by Otsu through his investigation of iniferters that were capable to initiate, transfer and terminate radical polymerization.[40, 41] DT techniques utilize chain transfer agents with exceptional high transfer constants best represented by xanthanes, macromolecular design via the interchange of xanthanes (MADIX) polymerization,[42, 43] or dithioesters.

Radical polymerizations carried out in the presence of thiocarbonylthio compounds which react by reversible addition-fragmentation chemistry are called RAFT polymerizations.[33, 44, 45] The use of a wide range of thiocarbonylthio compounds to control polymerizations has developed into a powerful synthetic tool for polymer chemists. The preparation of the corresponding chain transfer agents suffers from drawbacks such as the use of carbon disulfide in the syntheses and that the final RAFT-derived polymers are slightly colored and sometimes malodorous due to the presence of sulfur atoms. Nevertheless, despite being one of the most recent of the CRP systems, RAFT possesses a very high macromolecular engineering potential and is increasingly studied.[43]

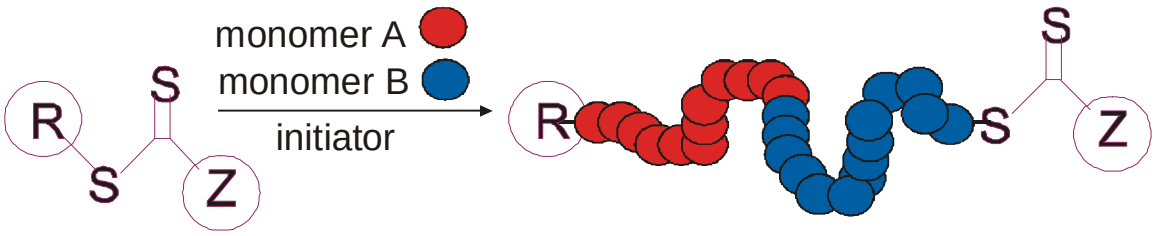

Scheme 1. *Schematic of the RAFT polymerization.*

Among the CRP techniques, RAFT polymerization appears to be the most versatile process in terms of the reaction conditions; the variety of monomers of which polymerization can be controlled, tolerance to functionalities, and the range of polymeric architectures that can be produced. Thus, it is expected that RAFT will be in the near future a synthetic tool as much used as ATRP, especially for preparing macromolecular amphiphiles.[46]

Simultaneous control of stereosequence and molecular weight distribution is one of the novelties in radical polymerization. Until now, CRP has been unsuccessful at attaining control over microstructure. Stereostructures (tacticities) are similar to those in conventional radical polymerization. Recently, however, there have been reports of simultaneous tactiticity and molecular weight control with certain monomers in ATRP and RAFT polymerizations.[47]

1.2.1.1 Mechanism of RAFT polymerization

The key feature of the mechanism of RAFT polymerization is a sequence of addition-fragmentation equilibria as illustrated in Scheme 2.[44] RAFT is based on the introduction of a small amount of thiocarbonylthio compound (a RAFT agent) in a conventional free radical polymerization. An external source of free radical, typically an azo compound, is required to initiate polymerization. The polymerization kinetics should be similar to conventional radical polymerization.[37] In the beginning of polymerization the radical initiator reacts with the monomer (M), forming the propagating radical (P_n•). This growing polymer chain reacts further with the C=S bond of the thiocarbonylthio compound [**1**] forming the intermediate (**2**). The fragmentation of the intermediate occurs reversibly towards the initial growing chain or to re-initiating group (R) from RAFT agent (or to a macro RAFT). This gives rise to a polymeric macro RAFT compound [**4**] and a new radical (R•). The new radical (R•) can initiate polymerization by reacting with monomer forming a new propagating radical (P_m•). This main equilibrium, a rapid exchange between the active propagating radicals (P_n• and P_m•) and the dormant polymeric thiocarbonylthio compounds (**5**), provides equal probability for all chains to grow. This procedure allows the production of polymers with narrow molecular weight distributions. Finally, at the end of the polymerization, most of the chains have a thiocarbonylthio end group.

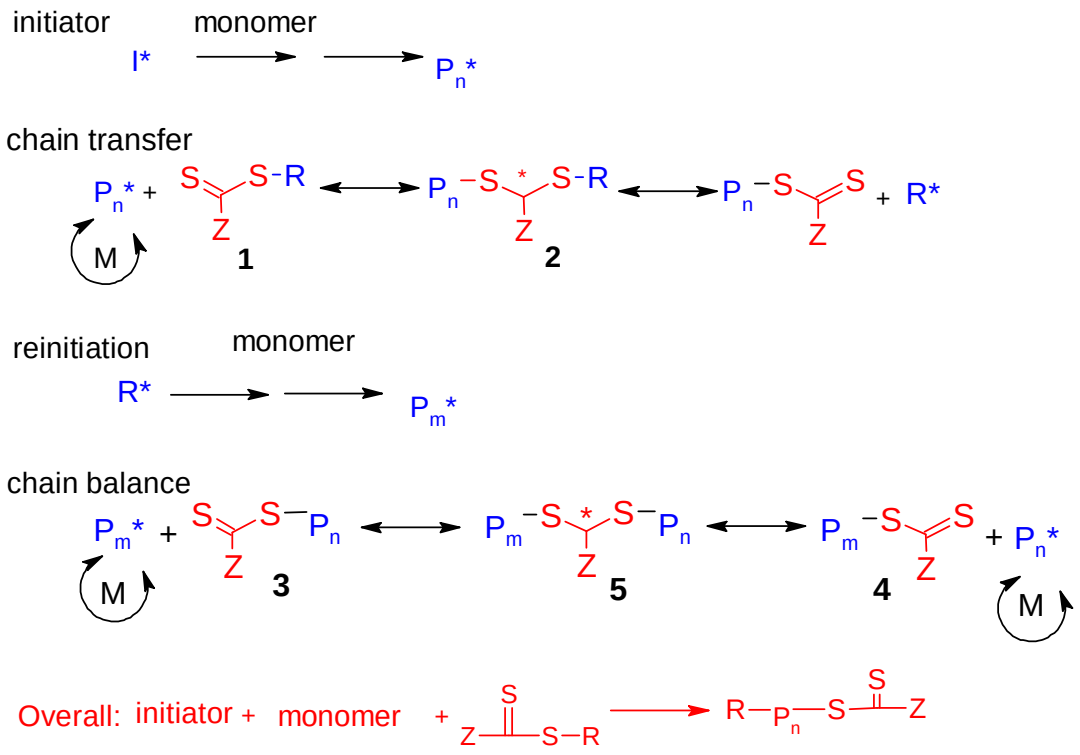

Scheme 2. *The mechanism of RAFT polymerization as it is generally accepted.*[44]

A wide variety of thiocarbonylthio RAFT agents have been reported. These include dithiobenzoates and other dithioesters, trithiocarbonates, xanthanes, dithiocarbamates and other compounds. The effectiveness of the RAFT agent depends on the monomers used, but is much more affected by the properties of the RAFT agent; the free-radical leaving group R and the group Z which strongly influences the stability of the thiocarbonyl double bond and the radical intermediate.[48] The influence of R and Z groups on the polymerization rates and selection of the appropriate RAFT agent for particular monomers is discussed in details in thorough reviews by Moad and Favier.[45, 49] In short, RAFT agents should have a reactive C=S double bond, intermediate radicals should fragment rapidly, the substituent R must be a good leaving group and radicals (R•) should efficiently re-initiate polymerization. Generally, the chain transfer coefficients decrease in the series dithiobenzoates > dithioesters > dithiocarbonates ≈ dithioalkanoates > xanthanes > dithiocarbamates. However, one should keep in mind that different monomers and different polymerization conditions, *e.g.* aqueous polymerizations or emulsion and mini-emulsion, require carefully selected RAFT agents.[46]

The theoretical number average molar weights in RAFT polymerization can be predicted using the equation: $M_{n,\ theor} = [M]_0 \times MW_{mon} \times conv / [CTA]_0 + MW_{CTA}$, where $[M]_0$, MW_{mon}, conv, $[CTA]_0$ and MW_{CTA} are the initial concentration of the monomer, molar mass of the monomer, fractional conversion, the initial concentration of the RAFT agent, and the molar mass of the RAFT agent, respectively.

1.2.1.2 RAFT polymerization in the presence of Lewis acid

Stereoisomerism in the structure of a polymer as a consequence of the polymerization reaction can strongly affect properties of the polymer. In a polymer of vinyl monomers CH2=CHX, the main-chain carbons have substituent group(s). Successive alignment of the side groups along the chain brings regularity or irregularity in the relative configurations. The simplest regular alignment is an isotactic structure, in which all the substituents are located on the same side of the planar zigzag chain. If the sidegroups of the successive stereocenters are randomly distributed on the two sides of the polymer chain, the polymer does not have order and is called atactic.[50]

The effective control of the stereochemistry in radical polymerization is hard to attain because the growing radical species is a planar-like sp^2-carbon, which induces a non-stereospecific propagation. Some stereospecific radical polymerizations have relied on the design of modified monomers but recently, more general methods applicable for usual vinyl monomers, have been developed.[51] Some control on the tacticity in radical polymerization has been achieved through the use of fluorinated alcohols as solvents.[52] Bulky fluoroalcohols or other polar solvents can interact with the polar substituents of the monomer units such as methacrylates, acrylamides and vinyl esters to induce stereospecific polymerization via the steric repulsion. Another method uses Lewis acids, such as magnesium halides and metal triflates.[53] Lewis acid works catalytically and leads to an isospecific radical polymerization via multiple site coordination to the polymer terminal. RAFT polymerization does not, by itself, give any control over stereochemistry. Thus, either the molecular weight or the tacticity can, at some extent, be controlled during the radical polymerizations while the simultaneous regulation of both has been difficult. One of the most significant features of CRPs is their tolerance to functionalities. This suggests that CRP can occur even in a polar solvent or in the presence of a Lewis acid. Thus, the stereocontrol in addition to the molecular weight

control is achievable, if the living and the stereospecific radical polymerizations could be combined in a way that one of the components does not disturb the control by the other.

The first report regarding the simultaneous control by the combination of living and stereospecific radical polymerizations was the RAFT polymerization of *N*-isopropylacrylamide in the presence of $Y(OTf)_3$.[54, 55] The obtained PNIPAMs had controlled molecular weights and high isotacticities, meso contents were 80-90% throughout the polymerizations. The dual control is most probably due to efficient interactions of the Lewis acid with the amide moieties in the polymer terminal and in the incoming monomer even in the presence of the RAFT agent. On the other hand, a fast conversion between the dormant dithioester group and the growing radical species is induced, without decomposition of the thioester group, even in the presence of $Y(OTf)_3$. This result was valuable as the first stereospecific living polymerization of NIPAM, because NIPAM cannot be polymerized by anionic polymerizations due to the presence of the amide proton. Hydrophilicity of PNIPAM can be controlled by changing its tacticity, which may be useful for the design of PNIPAM-based thermosensitive materials.[56] The combination of RAFT agents and metal triflates was also employed for the simultaneous dual control for *N*,*N*-dimethylacrylamide.[57]Another acrylamide, which contains a L-phenylalanine moiety, was also polymerized by this combination to give molecular weight-controlled polymers with a relatively high isotacticity (meso content 65%).[58] Also, RAFT copolymerizations of styrene and methyl methacrylate in the presence of Lewis acids were investigated and well-defined alternating copolymers were obtained.[59] Recently, the stability and effectiveness of the different RAFT agents in the presence of scandium triflate were thoroughly studied.[60]

It should be noted that by changing the amounts of the stereochemical mediators in RAFT polymerization, the stereoregulation can be modulated while maintaining the molecular weight control, because both controls are basically independent. This is opposite to stereospecific living ionic polymerizations, in which the counterion or the catalyst plays a dual role for both controls. Still, the degree of the chemical control in described combinations is lower than control in the stereospecific living polymerizations. Increasing the ratio of the Lewis acid produces more stereospecific polymers. Unfortunately, the addition of the Lewis acid also increases the rate of polymerization, leading to poorer control over the molecular weight and molecular weight distribution. Consequently, a different strategy for further developments in stereoregulation in CRP may be necessary in terms of the stereoregularity and versatility of the applicable monomers.[47]

1.2.2 Poly(N-isopropylacrylamide) – a thermally responsive polymer

Water-soluble polymers contain hydrophilic groups, which are able to interact strongly with water molecules. Polar groups in a polymer structure, such as amide groups, are prone to create water solubility. The formation of hydrogen bonds between hydrophilic groups and water molecules is the initial driving force for dissolution. On the other hand, vinyl backbones are hydrocarbons and thus hydrophobic. Water molecules re-orientate and form ordered hydration layers around the non-polar domains. The re-structuring of the water molecules is entropically unfavorable, and thus in order to minimize the entropic loss of the system, hydrophobic regions tend to segregate. This phenomenon is known as the hydrophobic effect and it induces hydrophobic interactions.[61]

The delicate balance between the interactions of hydrophilic and hydrophobic groups and water molecules determines the water solubility of polymers. Typically for some water-soluble polymers, this balance is gradually broken as temperature is increased. As a consequence, at higher temperatures a negative total entropy change controls the system over the enthalpy of the hydrogen bonding, and free energy change of the mixing becomes positive causing the phase separation. This kind of temperature dependent solubility raises fascinating opportunities. Based on the controllable change of the conformation of a polymer, various "smart" structures may be created that are sensitive to temperature. There are many polymers that exhibit thermally-induced precipitation, such as polymers with amide groups, ether groups or polymers with alocohol groups.

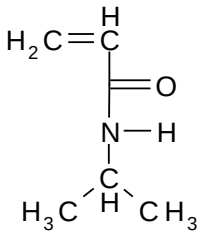

Scheme 3. *N-isopropylacrylamide*

Poly(*N*-isopropylacrylamide) (PNIPAM)[62-64] is one of the most extensively investigated synthetic water soluble temperature-responsive polymers, attracting great interest as a basic building block of smart materials.[65] This polymer is soluble in water below 32 ºC. When temperature is raised above the demixing temperature 32 ºC, the hydrophobic backbone and isopropyl groups of the polymer tend to associate. This causes intra- and intermolecular aggregation leading to the collapse of the PNIPAM chains and phase separation of the polymer. This temperature is also known as the cloud point. This phenomenon is reversible when the stimulus is reversed, although the rate of reversion is often slower as the polymer redissolves. If NIPAM monomer is copolymerized with more hydrophilic monomers, the cloud point increases and may even disappear. On the other hand, hydrophobic modification of PNIPAM decreases the cloud point and affects significantly the polymer demixing with increasing temperature.[66]

Owing to the progress in the CRP (1.2.1) it is relatively easy to synthesize block copolymers consisting of blocks with different responsive characters (e.g., temperature and pH sensitive blocks). Thus, amphiphilic and double hydrophilic block copolymers combining two stimuli sensitive polymers have attracted much attention.[67-69] In this work, PMAA-PNIPAM block copolymer represents this kind of composition. It is well-known that poly(methacrylic acid) (PMAA) can undergo a marked pH-induced conformational transition. At low pH, the PMAA chains adopt a compact structure due to hydrophobic interactions.[70, 71]

1.2.3 Block copolymer self-assembly

Block copolymers can simply be considered as being formed by two or more chemically homogeneous polymer fragments (blocks) joined together with covalent bonds. In the simplest case of two distinct polymers (A and B) linear diblock (AB) can be prepared. The micro phase separation of block copolymers has been intensively studied over recent decades and is relatively well understood.[72-74] This self-assembly is driven by an unfavorable mixing enthalpy and small mixing entropy, while the covalent bond connecting the blocks prevents macroscopic phase separation. In the bulk, the minority block segregates from the majority block forming regularly shaped nanodomains.[12] The shape of the nanodomains in a diblock copolymer is governed by the volume fraction of the minority block and block incompatibility. Thus, equilibrium morphologies such as spheres, hexagonal cylinders, lamellar or gyroidal layers can be formed.

In analogy to their bulk behavior, block copolymers also self-organize in solutions, typically in selective solvents, which solubilize one but not the other block.[75] Intensive studies on the self-assembly in selective solvents only began to emerge in 1995 with the discovery by Zhang and Eisenberg of multiple morphologies of block copolymers.[76] In the subsequent 10 years, much effort has been focused on the study of amphiphilic copolymers. Self-assembly of amphiphilic molecules and block copolymers in solution provides a versatile mechanism for the creation of multiple morphologies,[77] including spherical shells,[78] aggregates,[79] toroids,[80] vesicles,[10] tubes,[81] and several others. Because of their resemblance to many biological systems, the understanding of the mechanism for formation of various morphologies in block copolymer systems is significant to clarify the biological processes.

Various linear block copolymer architectures, such as ABA[82, 83] and ABC triblocks,[84] ABCA tetrablocks[85], multiblock copolymers[86] or telechelic polymers[87] have been show to produce multiple morphologies. However, most often morphologies are kinetically controlled by variation of solution conditions such as solvent composition, concentration or pH.[88] Thus, morphology can be altered without having to change the chemistry of the block copolymer. Such assemblies are kinetically trapped and unable to thermodynamically equilibrate. Temperature-dependent assemble/disassembly of thermoresponsive copolymers have also been demonstrated, where reversible morphological transitions are induced solely by temperature.[89, 90]

1.2.4 Polymer protected gold nanoparticles

Interest in the synthesis and properties of nanoscopic colloidal metal particles and metal clusters has increased over the last few years because of their unique properties.[19, 91] Gold nanoparticles, especially, have attracted great interest due to the fact that gold is the most stable and inert noble metal possessing unique surface properties and good conductivity.[20, 92, 93] Inspired by the synthetic advances in preparing alkane-thiol-protected gold particles,[94] functional polymers and oligonucleotides have been used to protect gold nanoparticles.[95]

In the "grafting-to" strategy to prepare polymer protected gold clusters, polymers end-capped with a thiol group or containing a disulfide unit have been used instead of alkanethiol ligands.[96-99] The "grafting-to" strategy is an especially useful synthetic route to prepare polymer stabilized gold clusters, when combined with RAFT polymerization which enables the control of the molecular weight and molecular weight distribution of the polymers ligands.[100]

Polymer protected gold nanoparticles are prone to flexible material design and colloidal particles offer a route to the simple assembly of complex structures. Also, stimuli-sensitive polymer such as PNIPAM, which is directly bound to the metal surface, is expected to be capable of modulating the intimate surrounding of particles that determines many of the properties of the nanoparticles.

1.3 Objectives of the study

The major objective of this work was to synthesize novel, tailor-made PNIPAM based thermally responsive block copolymers by controlled RAFT polymerization. The purpose was to show how these precisely synthesized amphiphilic polymers could be utilized to obtain organized, functional systems. Accordingly, the overall study is divided into a detailed synthesis part and the discussion about different stimuli-sensitive self-organized materials.

First, RAFT polymerization was used to build up series of diblock copolymers comprising of a hydrophilic PNIPAM block and a hydrophobic block, either PS or P(*t*-BMA). We wanted to study aqueous solutions of the polymers to observe what kind of structures could be formed. Formation of polymeric nanoparticles with thermally responsive character in water was verified. Hydrophobic sequences alter the temperature range of dehydration and it has been of interest to find out how they affect the phase transitions in the case of micelle type particles.

Secondly, NIPAM A-B-A stereoblock polymers where an atactic PNIPAM block acts as a hydrophile and a short isotactic PNIPAM as a non water-soluble block were synthesized. Thus, these stereoblock polymers may be regarded as amphiphilic block copolymers and can be compared to block copolymers of PNIPAM and PS. The self-organization and phase-transition behaviour of A-B-A stereoblock polymers of PNIPAM in aqueous solution have been studied.

Thirdly, a series of triblock copolymers, PS-PNIPAM-PS, was prepared. The weight fraction of PS was varied in order to investigate the phase behavior in bulk and to design novel aqueous hydrogels based on lamellar, gyroid, cylindrical, and spherical block copolymer morphologies.

Finally, PNIPAM homo polymer and PMAA-PNIPAM block copolymer were used to passivate gold nanoparticles in a one-pot synthesis, where the polymer is bound to the gold surface by a sulphur bridge. The properties of the gold nanoparticles protected with stimuli-sensitive diblock copolymers can be modified varying pH and temperature of aqueous dispersions of the particles.

2 EXPERIMENTAL

This section summarizes the synthetic methods and the characterization of all polymers, homopolymers and block copolymers used during this work. Then, the methods to prepare self-organized samples are described, in aqueous solutions and in solid state. Also, preparation of the polymer protected gold nanoparticles is described.

2.1 Polymer synthesis

2.1.1 Raft agents

The synthesis of the RAFT polymers was started by preparation of three different RAFT agents. The synthetic routes of monofunctional RAFT agents, 2-phenyl-prop-2-yl dithiobenzoate (cumyl dithiobenzoate, CDB)[44] and 4-cyanopentanoic acid dithiobenzoate (CPA) are described elsewhere.[101] CDB is water insoluble due to the hydrophobic end groups. A bifunctional S,S'-bis(α,α'-dimethyl-α"-acetic acid)-trithiocarbonate (BDAT) is water-soluble due to carboxylic acid end groups. BDAT was prepared by the method of Lai et al.[102]

cumyl dithiobenzoate (CDB)

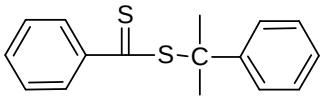

4-cyanopentanoicacid dithiobenzoate (CPA)

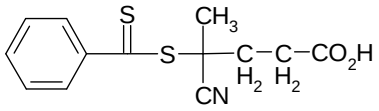

S,S'-bis(α,α'-dimethyl-α"-acetic acid)-trithiocarbonate (BDAT)

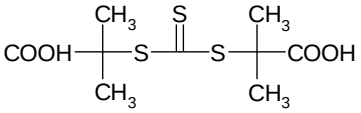

Scheme 4. *RAFT agents utilized in this work.*

2.1.2 RAFT homopolymerizations

Typical homo polymerization procedures are described and polymerization conditions are listed in Table 1.

2.1.2.1 Kinetic measurements of N-isopropylacrylamide polymerization (Paper V)

The efficiency of BDAT in NIPAM polymerizations in the presence of a Lewis acid has not been studied before. Thus, polymerization rates with and without $Y(OTf)_3$ were compared. For each kinetic plots, several separate polymerizations with and without Lewis acid were performed. ^1H NMR (200 MHz) of the reaction mixture was taken before removal of the solvent to determine conversions. The solvent was evaporated at ambient temperature under vacuum and samples were analyzed directly by SEC. In a typical procedure to prepare isotactic PNIPAM, AIBN (1:4 molar ratio to RAFT agent), BDAT (1:50 - 1:250 molar ratio to NIPAM monomer), $Y(OTf)_3$ (1:20 molar ratio to NIPAM monomer) and NIPAM (2.0 M) were dissolved into a mixture of methanol and toluene (1:1 v/v). The solution was degassed by three successive freeze-thaw cycles in a Schlenk line. All polymerizations were conducted at 60 °C.

2.1.2.2 Polymerization of N-isopropylacrylamide (Papers I, II & IV)

Polymerizations of atactic NIPAM were carried out in dioxane. Samples were freeze-thawed to remove oxygen and placed in a oil bath at 60 °C. PNIPAM was purified by precipitation to diethyl ether and water heated above 40 °C.

2.1.2.3 Polymerization of styrene (Papers II & IV)

In a typical styrene polymerization, RAFT agent, AIBN and styrene were dissolved in 1,4-dioxane. Solution was degassed by three freeze-pump-thaw cycles, the vessel was sealed under vacuum and placed in a thermostatically controlled oil bath (60 or 70 °C) The polymer was precipitated in cold methanol and purified by repeated precipitations.

2.1.2.4 Polymerization of tert-butylmethacrylate (Papers II & III)

A solution of *t*-BMA, CDB and AIBN in 1,4-dioxane was added to a reaction vessel. System was degassed by three freeze-pump-thaw cycles, sealed under vacuum and placed in a thermostated oil bath (70 °C) for 46 hours. The polymer was precipitated in a water-methanol mixture (1:4) and the product was dried under vacuum.

2.1.3 RAFT block copolymerizations

Procedures for different block copolymers are shortly described. Details of all block copolymerizations and characteristics of the products are listed in Table 2.

2.1.3.1 Synthesis of poly(tert-butylmethacrylate-block-N-isopropylacrylamide) (Papers II & III)

A well characterised P(*t*-BMA) RAFT macroinitiator was dissolved in 1,4-dioxane before adding NIPAM monomer and AIBN. The system was freeze-thawed and placed in a thermostated oil bath (70°C) for 44 hours. The polymers were precipitated in water/methanol (1:1) mixtures. Purification was repeated by dissolving polymer in chloroform and precipitating in water/methanol.

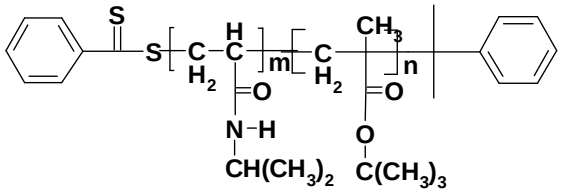

Scheme 5*. Poly(tert-butylmethacrylate-block-N-isopropylacrylamide)*

Table 1. *Characteristics and polymerization conditions of homopolymerizations.*

Polymer	paper	monomer A (concn, solvent, temperature)	RAFT[a] (mM)	AIBN (mM)	time	M_n (g mol^{-1})	M_w/M_n
PNIPAM-5400	I	NIPA (1.8 M, dioxane, 60 °C)	CTA (9.0)	0.6	48h	5 400	1.13
PNIPAM-24300	V,VI	NIPA (2.0 M, dioxane, 60 °C)	BDAT(8.0)	2.0	5h	24 300[b]	1.22[b]
PNIPAM-i4200	V,VI	NIPA (2.0 M, methanol/toluene, 60 °C)	BDAT(40.0)[c]	10.0	70min	4 200[b]	1.46[b]
PNIPAM-i10200	V	NIPA (2.0 M, methanol/toluene, 60 °C)	BDAT(16.0)[c]	4.0	30min	10 200[b]	1.57[b]
P(t-BMA)-19400	II,III	t-BMA (6.0 M, dioxane, 70 °C)	CDB(12.3)	1.3	46h	19 400	1.15
PS-8000	II	styrene (bulk, 60 °C)	CTA(16.5)	2.4	23h	8 000	1.05
PS-5200	II	styrene (2.9 M, dioxane, 60 °C)	CTA (4.7)	0.5	48h	5 200	1.08
PS-7200	IV	styrene (4.7 M, THF, 60 °C)	BDAT (2.9)	0.6	20h	7 200	1.21
PS-27600	IV	styrene (2.2 M, dioxane, 70 °C)	BDAT (1.3)	0.8	48h	27 600	1.50
PS-41200	IV	styrene (2.2 M, dioxane, 70 °C)	BDAT (0.7)	0.8	48h	41 200	1.31
PS-17700	IV	styrene (2.2 M, dioxane, 70 °C)	BDAT (0.8)	0.8	48h	17 700	1.57
PS-41000	IV	styrene (2.2 M, dioxane, 70 °C)	BDAT (0.7)	0.8	48h	41 000	1.38
PS-37000	IV	styrene (2.9 M, dioxane, 70 °C)	BDAT (0.9)	0.9	72h	37 000	1.55

[a] CTA, 4-cyanopentanoic acid dithiobenzoate; CDB, cumyl dithiobenzoate; BDAT, S,S'-bis(α,α'-dimethyl-α''-acetic acid)-trithiocarbonate. M_n and M_w/M_n are determined by SEC with THF using calibration with PS standards, except [b] where the measurements were conducted in DMF (0.1 M LiCl) with poly(methylmethacrylate) standards. [c] including 0.1 M of $Y(OTf)_3$.

Table 2. *Characteristics and polymerization conditions of block copolymerizations.*

polymer	A	block B, NIPAM (concn, solvent, temp, time)	block A (macroRAFT) (concentration)	M_n[a] ($g\ mol^{-1}$)	M_w/M_n[b]
PS_{48}-$PNIPAM_{346}$ (A)	II	(1.9 M, dioxane, 60 °C, 42h)	PS-5200 (4.5 mM)	44 300	1.34
PS_{75}-$PNIPAM_{118}$ (B)	II	(1.9 M, dioxane, 60 °C, 42h)	PS-8000 (6.3 mM)	21 400	1.15
P(*t*-BMA)$_{135}$-$PNIPAM_{123}$(C)	II,III	(0.9 M, dioxane, 70 °C, 44h)	P(t-BMA)-19400 (5.6 mM)	33 300	1.13
PS_{33}-$PNIPAM_{161}$-PS_{33}	IV	(1.0 M, dioxane,70 °C, 24h)	PS-7200 (1.6 mM)	25 400	1.23
PS_{33}-$PNIPAM_{245}$-PS_{33}	IV	(1.0 M, dioxane,70 °C, 24h)	PS-7200 (0.8 mM)	34 900	1.26
PS_{33}-$PNIPAM_{294}$-PS_{33}	IV	(1.0 M, dioxane,70 °C, 24h)	PS-7200 (0.5 mM)	40 500	1.44
PS_{131}-$PNIPAM_{805}$-PS_{131}	IV	(1.1 M, dioxane,70 °C, 20h)	PS-27600 (1.2 mM)	118 300	1.51
PS_{197}-$PNIPAM_{573}$-PS_{197}	IV	(0.9 M, dioxane,70 °C, 18h)	PS-41200 (1.2 mM)	106 000	1.52
PS_{84}-$PNIPAM_{402}$-PS_{84}	IV	(2.2 M, dioxane,70 °C, 18h)	PS-17700 (2.8 mM)	63 200	1.41
PS_{196}-$PNIPAM_{438}$-PS_{196}	IV	(1.0 M, dioxane,70 °C, 24h)	PS-41000 (1.6 mM)	90 500	1.26
PS_{176}-$PNIPAM_{244}$-PS_{176}	IV	(0.7 M, dioxane,70 °C, 18h)	PS-37000 (1.3 mM)	64 600	1.27
PNIPAM i2-a40-i2	V	(2.0 M, meth./tol., 60 °C, 17h)	PNIPAM-i4200 (5.6 mM)	44 200	1.29
PNIPAM i2-a28-i2	V,VI	(2.0 M, meth./tol., 60 °C, 17h)	PNIPAM-i4200 (8.0 mM)	32 200	1.29
PNIPAM a12-i5-a12	V	(2.0 M, meth./tol., 60 °C, 155min)	PNIPAM-24300 (26.6 mM)	29 300	1.32
PNIPAM a12-10-a12	V,VI	(2.0 M, meth./tol., 60 °C, 165min)	PNIPAM-24300 (26.6 mM)	34 300	1.37
PNIPAM i5-a70-i5	V	(2.0 M, meth./tol., 60 °C, 17h)	PNIPAM-i10200 (3.2 mM)	80 200	1.31
PNIPAM i5-a28-i5	V	(2.0 M, meth./tol., 60 °C, 17h)	PNIPAM-i10200 (8.0 mM)	38 200	1.20

[a] M_n of the A-B block copolymer determined with ^{1}H NMR spectroscopy for block copolymers of styrene and NIPA, otherwise (stereoblock copolymers) by SEC, in DMF (0.1 M LiCl) with poly(methylmethacrylate) standards. [b] Determined using SEC

2.1.3.2 Syntheses of the block copolymers of styrene and N-isopropylacrylamide (Papers II & IV)

The PS macro RAFT agent was dissolved in 1,4-dioxane before adding NIPAM and AIBN. The mixture was stirred for 30 min at room temperature to dissolve all the components. The solution was degassed by three successive freeze-pump-thaw cycles. The polymerization reaction was started by placing the mixture in an oil-bath at 70 °C. The product was purified by two reprecipitations from THF into diethyl ether and cold water. The product was freed from the homopolymer PNIPAM by centrifugation at 29 °C (45 min, 5000 rpm).

2.1.3.3 A-B-A stereo block polymers of N-isopropylacrylamide (Paper V)

Two isotactic PNIPAMs with varying molar masses and one atactic PNIPAM were used as macro RAFT agents in the stereoblock polymerizations. A typical polymerization procedure was similar to homopolymerization (2.1.2.1). Polymers were extensively purified by precipitating from THF to diethyl ether and from methanol to water.

2.1.4 Preparation of poly(methacrylic acid-*block*-N-isopropylacrylamide) *(Paper III)*

PMAA-PNIPAM was prepared by hydrolyzing the P(*t*-BMA)-PNIPAM under acidic condition. Polymer was dispersed in a 4.0 M HCl solution. The reaction mixture was heated at 80 °C for 24 h. Then, the solution was dialyzed in water for several days. The ^{1}H NMR spectrum of the resulting PMAA-PNIPAM in D_2O showed the disappearance of the *tert*-butyl resonance at δ = 1.40 ppm. Hydrolysis of PNIPAM to poly(acrylamide) was not observed.

2.2 Preparation of block copolymer samples

2.2.1 Preparation of aqueous polymer solutions *(Papers II, V, VI)*

The capability of the diblock copolymers to build up micellar structures was studied by carefully transferring the polymers from an organic solvent into water. PS-PNIPAM diblock copolymers were dissolved in N,N-dimethylacetamide (DMA, 0.5 wt %), which is a common solvent for both blocks. Deionised water was added dropwise to the solutions with vigorous stirring. 15 – 25 wt % of water was added depending on polymer. The quality of the solvent became gradually poorer for the hydrophobic blocks, this causing the aggregation of the hydrophobic blocks observed as the turbidity of the solutions. The resulting slightly opaque solutions were placed in dialysis bags (MW cut-off:3500) and dialysed against purified water to remove DMA.

PNIPAM stereoblock copolymers disperse spontaneously in water, forming micelle aggregates, even if isotactic PNIPAM is water insoluble.

2.2.2 **Preparation of solid samples** *(Paper IV)*

Polymers were dissolved in THF to yield 1.0 wt-% solutions. The solvent was evaporated at room temperature, the samples were dried in a vacuum at room temperature for 4-6 hours, and annealed at ca. 180 °C under a high vacuum 10^{-8} mbar for 3-4 days.

2.3 Preparation of gold nanoparticles *(Papers I & III)*

RAFT polymers terminated with a dithioester group can be directly employed in the synthesis of gold nanoparticles. $LiB(C_2H_5)_3H$ is a strong base and reduces $HAuCl_4$ to Au(0) and simultaneously hydrolyzes dithioester to a thiol. Thiols react quickly with gold surface and polymers form protecting layers on gold nanoparticles.

To a solution of 0.1 mmol of $HAuCl_4 \cdot xH_2O$ in 10 mL of anhydrous THF was added 0.01 mmol of PMAA-PNIPAM in 10 mL of methanol (the molar ratio polymer/$HAuCl_4 \cdot xH_2O$ = 1/10) or 0.02 mmol of PNIPAM in THF (the molar ratio polymer/$HAuCl_4 \cdot xH_2O$ = 1/12). The mixture was stirred for 30 min in an ice bath. Then, 1.0 mL of 1.0 M solution of $LiB(C_2H_5)_3H$ in THF was added dropwise for 2 min to the vigorously stirred solution. The solution mixture turned immediately purple and was stirred in an ice bath for a further 4 h. The resulting mixtures were simultaneously purified and fractionated through centrifugation. In addition, dispersions were ultrafiltrated to separate all the unreacted polymers. The aqueous dispersions were frozen and lyophilized.

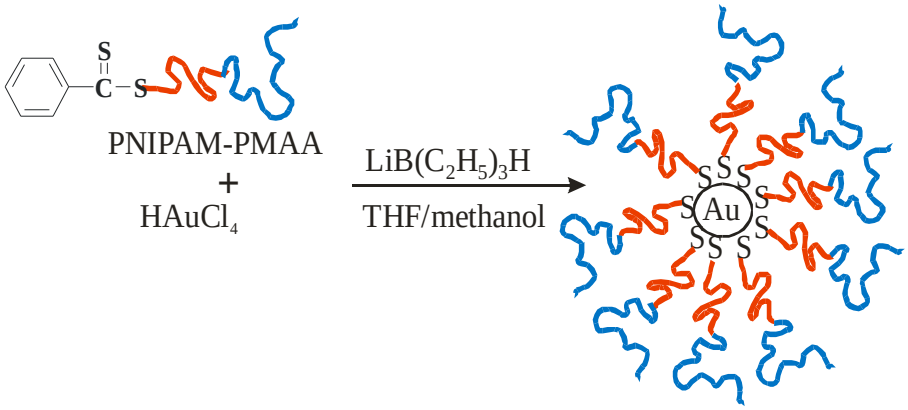

Scheme 6*. One-step synthesis of Au-PNIPAM-PMAA with a gold core, a PNIPAM inner shell and a PMAA corona.*

2.4 Instrumentation

The experimental details of the characterization and experimental methods can be found in the original paper as follows:

The molar masses (M_n) and molar mass distributions (M_w/M_n) were determined using Waters SEC equipment with Styragel columns, a Waters 2410 refractive index detector and Waters 2487 UV detector.[I, II, III, IV, V]

M_n of the short PNIPAM samples were also determined by on a Bruker Microflex MALDI-TOF mass spectrometry equipped with 337 nm N_2 laser.[V]

The structure and purity of the polymers, as well as conversion of the polymerizations, were ascertained with a 200 MHz Varian Gemini 2000 ^{1}H NMR spectrometer.[I,II,III,IV,V] In addition, a Varian Inova 500 ^{1}H NMR spectrometer and a Varian UNITYInova ^{13}C NMR spectrometer at 80 °C were used in the tacticity studies.[V]

The amount of polymer ligands on the gold core surface was determined using a Mettler Toledo TGA 850.[I, III]

Differential scanning calorimetry (DSC) measurements on dry polymer samples were performed with a Mettler 822e differential scanning calorimeter to determine glass transition temperatures (T_g).[II, V]

Hydrodynamic radii (R_h) of the aggregates/polymers/nanoparticles were measured using dynamic light scattering (DLS).[I, II, III, VI] DLS, and static light scattering, SLS,[II, VI] experiments were conducted with a Brookhaven Instruments BI-200SM goniometer, a BI-TurboCorr digital auto/crosscorrelator, and a BI-CrossCorr detector, including two BI-DS1 detectors. Phase transition temperatures were also observed by DLS.[VI]

The specific refractive index increment (d*n*/d*c*) values needed for light scattering measurements were determined with Billingham & Stanley Abbe60/ED laser differential refractometer.[II, VI]

Surface plasmon bands of gold nanoparticles were measured by Shimadzu UV-1601PC spectrophotometer.[I, III] UV-vis spectrophotometry was also used in turbidity measurements.[V,VI]

Thermal transitions of dilute aqueous solutions of polymers were measured with a Microcal VP-DSC microcalorimeter. [II, III, V, VI]

High resolution transmission electron microscopy (HRTEM), FEI Tecnai 12 TEM operating at an accelerating voltage of 120 kV, was used for determination of the size distribution and the mean diameter of gold nanoparticles [I,III] and the morphologies of the bulk polymer samples.[IV]

Cryo-TEM microscopy, FEI Tecnai F20 electron microscope at 200kV under low dose conditions, was used to visualize aqueous polymer solutions.[II]

3 RESULTS AND DISCUSSION

3.1 Polymer synthesis

At the time this work was started, CRP methods were not practiced in Finland. As a consequence, the work was started with testing different reaction conditions (solvents and ways to remove oxygen) and various RAFT agents. CDB was selected for a RAFT agent, since it was reported to be able to control NIPAM polymerization.[103] Dithioacetate and dithiobenzoate where also tested, but they appeared to be inefficient in the polymerization of NIPAM. CPA was chosen as another RAFT agent as it was shown to be to be effective in block copolymerizations involving styrene.[104] In addition, carboxylic acid end group enables further functionalization of the polymer, thus, BDAT was used to prepare triblock copolymers.

In NIPAM and styrene polymerizations, the best results were obtained using freeze-thaw cycles with dioxane as a solvent. Thus, the most of the polymers studied in this work were synthesized under these conditions, except stereo controlled polymerizations of NIPAM for which methanol/toluene mixture was chosen as a solvent based on literature. It was shown in this work that NIPAM and styrene can be copolymerized efficiently by RAFT. Of the studied RAFT agents, trithiocarbonate was shown to be the most suitable chain transfer agent for use in RAFT polymerization when $Y(OTf)_3$ was present.

3.1.1 Block copolymerizations of N-isopropylacrylamide and styrene *(Papers II & IV)*

The first part of this work was to prepare amphiphilic diblock copolymers which self-assemble to form stimuli-responsive porous membranes. We also wanted to study self-organization of the same polymers in aqueous solutions. Thus, PNIPAM and polystyrene were chosen.

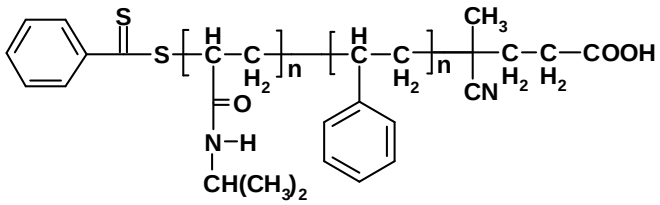

Scheme 7. *Poly(styrene-block-N-isopropylacrylamide)*

In general it is preferable to start block copolymerization with the monomer having the lowest chain transfer constant. Thus, in this work, a polystyrene block was prepared first. Next, monodisperse PS (or P(*t*-BMA)) polymers were used as macro RAFT agents in the syntheses NIPAM. As a result, well-defined diblock copolymers with appropriate hydrophilic/hydrophobic balance were successfully prepared.

The growth of the block copolymers was confirmed by SEC. Polymerizations fulfilled one criterion of controlled polymerizations, namely the average molar masses (M_n) obtained by SEC were usually in a good agreement with theoretical values. However, SEC results for the block polymers with PNIPAM blocks are assumed to be

somewhat inaccurate, because of problematic behavior of PNIPAM in SEC measurements.[103, 105] In the beginning of the work we used typical THF eluent in SEC measurements. Thus, polymers were also analyzed by ^{1}H NMR and the M_n of the block copolymers were calculated from the integrals of the characteristic peaks in ^{1}H NMR. Later, when stereoblock polymers were studied, SEC measurements were conducted in DMF (0.1 M LiCl) with poly(methylmethacrylate) standards.

The bifunctional BDAT was used in the triblock copolymer synthesis. Synthesized block copolymers using BDAT were A-B-A triblock polymers with PS as an A block and PNIPAM as a B block. SEC showed that the PS block was fully incorporated into the triblock copolymer, and monomodal SEC trace proves pure triblock copolymer (Figure 1).

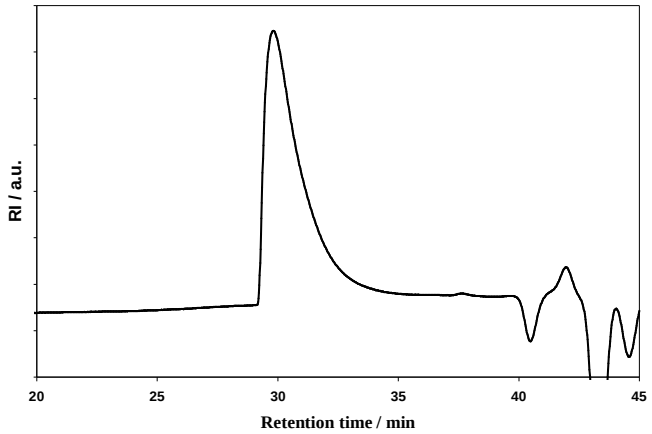

Figure 1. *SEC trace of PS_{33}-$PNIPAM_{245}$-PS_{33} (M_n = 34 900 g/mol). For details on molecular weight see Table 2.*

3.1.2 Tacticity control in the RAFT polymerization of N-isopropylacrylamide *(Paper V)*

The effieciency of BDAT in NIPAM polymerizations in the presence of a Lewis acid had not been studied before. Based on the literature, $Y(OTf)_3$ was chosen as a suitable Lewis acid.[54] Polymerization rates with and without $Y(OTf)_3$ were compared and thus, $Y(OTf)_3$ concentration was kept constant. The Lewis acid noticeably increases the rate of polymerization (see Figure 2). Figure 2 shows a typical first-order time-conversion kinetics plot for the PNIPAM RAFT polymerization,[105] certifying that despite the high polymerization rate, at least a moderate molecular weight control is achieved.

In the stereo controlled polymerizations the control over the molar mass decreases, especially at low conversions (Figure 3). However, despite this slight lack of control, at high conversion the molar mass of the isotactic PNIPAM is close to the theoretical M_n. The decrease of the polydispesity index (PDI) with conversion indicates of good controllability as well (Figure 3) and the polydispersity is actually slightly better than in the presence of RAFT agents reported previously.[55] This is mainly because trithiocarbonate is more stable compared to dithiobenzoates in the presence of the Lewis acid.[106] M_w/M_n for isotactic PNIPAM was around 1.5 and for atactic PNIPAM, in the range of 1.2-1.3. As a summary, BDAT has proven to be an efficient RAFT agent in stereocontrolled polymerizations of NIPAM even if $Y(OTf)_3$ slightly decreases the control over the molar mass due to a higher reaction rate.

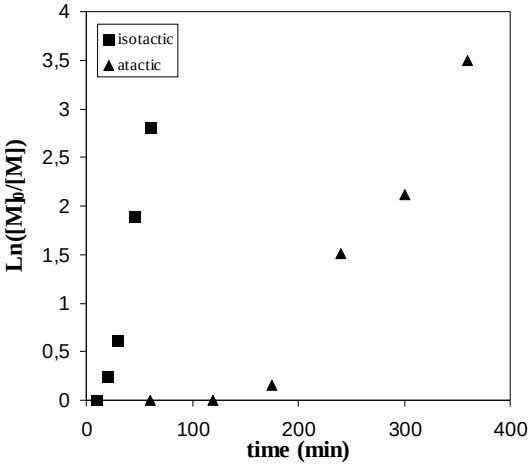

Figure 2. *Pseudo first-order rate plot of $ln([M]_0/[M]$ versus time for the NIPAM (2.0 M in methanol/toluene, 1:1 v/v) polymerizations performed at 60 °C in the presence of BDAT (8.0 mM) as RAFT agent, AIBN (2.0 mM) as initiator with ($Y(OTf)_3$ 0.1 M, ■) and without Lewis acid (▲).*

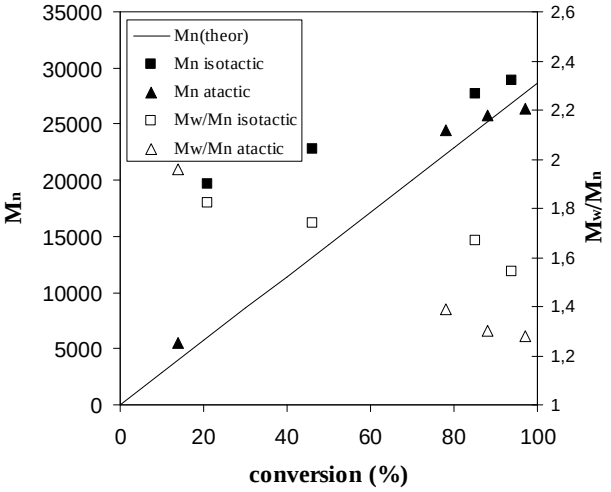

Figure 3. *Evolution of experimental molecular mass, M_n and polydispersity with theoretical M_n for the polymerization of PNIPAM (2.0 M in methanol/toluene, 1:1 v/v) performed at 60 °C in the presence of BDAT as a RAFT agent (8.0 mM), AIBN (2.0 mM) as initiator and with [$Y(OTf)_3$ 0.1 M, M_n (■), M_w/M_n (□)] and without Lewis acid [M_n (▲), M_w/M_n (Δ)].*

Next, an isotactic and an atactic PNIPAM prepolymer were used as macro RAFT agents. Accordingly, four block copolymers were obtained with isotactic PNIPAM blocks at the both chain ends - as low molar mass stickers. Similarly, an atactic PNIPAM was used as a macro RAFT agent and in those cases the isotactic block was set into the middle part of the block polymer. Both atactic and isotactic PNIPAMs can be used as macro RAFT agents. The efficient chain growth (increase of molar mass) during block polymerization was verified using SEC (Figure 4). SEC results were also well in accordance with the theoretical values.

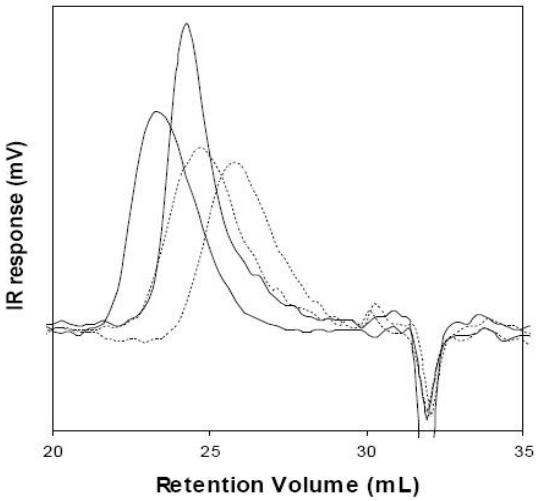

Figure 4. *SEC traces (RI) of PNIPAM prepolymers and stereoblock polymers. Prepolymers, atactic PNIPAM (24 300 g/mol) and isotactic PNIPAM (10 200 g/mol), are represented by dashed line. Corresponding stereoblock polymers (solid lines) from left to right are a i5-a70-i5 and a12-i10-a12.*

The successful control of tacticity was proven by spectroscopy in the ^{13}C NMR. The amount of meso dyads at 41-42 ppm for the isotactic PNIPAM was notably higher than that observed for the atactic polymer (Figure 5). An increase in isotacticity of the block polymers was similarly observed compared to atactic PNIPAM. Also, another difference in the ^{13}C spectra between atactic, isotactic and stereoblock PNIPAMs was detected in the β-carbon signal at 34.4 ppm.

The ^{1}H NMR (Figure 6) showed an increase in the intensity of the methylene protons at 1.6 ppm (meso dyad peak). The increasing of meso dyad peak indicates an increase in the isotactic content of the polymer.[54, 107] As the amount of isotactic regions increased, the racemo dyad peak around 1.45 ppm decreased. The decrease of the racemo peak and a slight shift of the meso dyad peaks to lower chemical shift values as isotactic content increases, revealed another meso dyad signal at 1.35 ppm. This meso dyad peak overlaps with the racemo peak in the spectrum of atactic PNIPAM and can only be seen in the spectra of isotactic PNIPAM. Unfortunately, the overlapping of the meso dyad peak with the racemo peak prevented the exact quantitative determination of the degree of isotacticity of the polymers. However, we can qualitatively conclude that isotactic PNIPAM is insoluble in water at room temperature, indicating that racemo content is at least 70%.[56, 107] As all the isotactic blocks have been synthesized under identical reaction conditions, we can safely assume, that the meso content of all isotactic blocks presented in this work are comparable and are of the order 70-80 %.

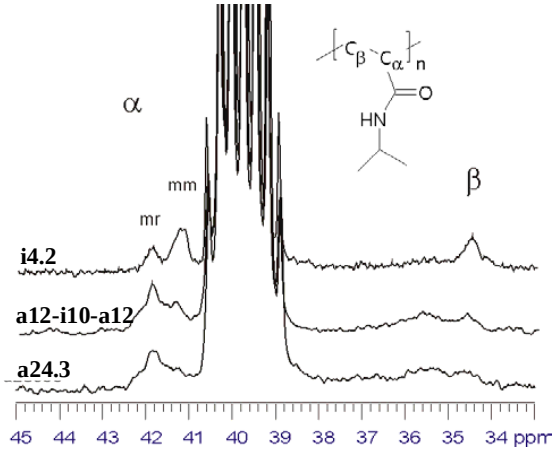

Figure 5. *Expanded ^{13}C NMR (75 MHz, DMSO-d6, 80 °C) spectra of isotactic, stereoblock and atactic PNIPAM.*

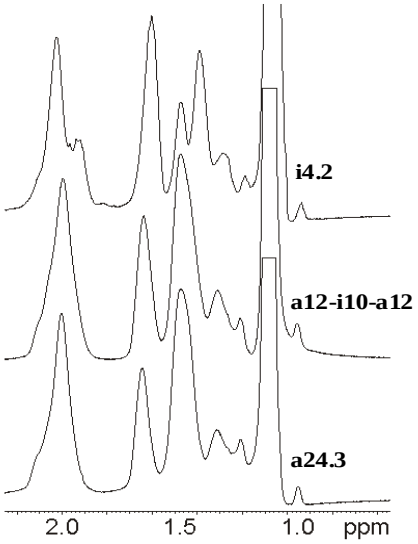

Figure 6. *Expanded ^{1}H NMR (500 MHz, DMSO-d6, 80 °C) spectra of main-chain methane and methylene groups of PNIPAM in isotactic, stereoblock and atactic polymer*

3.2 Block copolymers in the solid state

3.2.1 Differential scanning calorimetry measurements of block copolymers

The glass transition temperature of the block copolymers was measured to get an estimate of the compatibility of the chemically different blocks.

3.2.1.1 The glass transition of poly(styrene-block-N-isopropylacrylamide) (Paper II)

The glass transition temperatures of the diblock copolymers of PS/P(*t*-BMA)-PNIPAM are collected in Table 3. The two different blocks phase separated, since there were two separate T_gs corresponding to pure homopolymer segments. In the case of mixtures of compatible polymers, the two T_gs should merge and the glass transition temperatures should change with block ratio of the segments. As expected in the case of block copolymers containing PS blocks, the chemically different blocks were phase separated. The T_g of polystyrene was slightly higher in the block copolymers compared to that of pure PS, due to the motional restrictions imposed by PNIPAM**.** The methacrylate block despite of its higher polarity compared to polystyrene, phase separated in the same way.

Table 3. *The glass transition temperatures measured by DSC.*

sample	T_{g1} (°C)	T_{g2} (°C)
PS_{48}-$PNIPAM_{346}$	106.0	137.1
PS_{75}-$PNIPAM_{118}$	107.3	133.3
$P(t\text{-}BMA)_{135}$-$PNIPAM_{123}$	118.1	134.3

T_{g1} is for hydrophobic block T_{g2} is for PNIPAM block

3.2.1.2 The glass transition of poly(N-isopropylacrylamide) stereoblock polymers (Paper V)

The T_gs of the stereoblock PNIPAMs and the corresponding macroinitiators are shown in table 4. T_g was determined as an average of three consecutive runs on each sample, reproducibility of the T_g being within ±0.8 ºC. T_g for longer atactic PNIPAM sample was observed to be above 130 °C as in the case of PS-PNIPAM. The molecular mass had an effect for the atactic PNIPAM only with the lowest molar mass (M_n = 5500 g/mol); the T_g value was 7 ºC lower than for the others. On the other hand, T_g of isotactic PNIPAM was more molar mass dependent. When the molar mass of isotactic PNIPAM was < 10^4 g/mol, T_g was substantially lower than that of atactic PNIPAM. Instead, when the molar mass increased above 2.5 * 10^4 g/mol T_g increased to 158 °C. Hence, the glass transition temperature of PNIPAM was varied between 115 and 158 °C by adjusting the isotacticity.

Table 4. *The glass transition temperatures measured by DSC.*

sample	T_g (°C)
a24.3	132.8
a5.5	124.9
i4.2	115.3
i10.2	118.8
i28.9	157.6
a12-i10-a12	130.2
i2-a28-i2	128.0
i5-a28-i5	124,8
mix (1/1) a24.3+i28.9	142.4

a = atactic, i = isotactic

Interestingly, only one glass transition was observed for all stereoblock polymers. This observation was completely opposite to the case of PS-PNIPAM block copolymers. One T_g means that PNIPAMs with different tacticities are completely miscible and do not phase separate in bulk. Miscibility was proved by a simple test. Atactic PNIPAM (M_n = 24 300 g mol^{-1}, T_g = 132.8 °C) and isotactic PNIPAM (M_n = 28 900 g/mol, T_g = 157.6) were mixed in a common solvent (THF, 1/1 mass ratio) and dried. This mixture also showed only one T_g, 142 °C. This phenomenon may affect the phase behavior of stereoblock polymers compared to other amphiphiles.

The T_gs of PNIPAM stereoblock polymers may be varied by varying the mutual lengths of the atactic and isotactic blocks. Thus, the T_gs of the studied stereoblock polymers varied depending on the isotactic block length although the differences were relatively small (2-8 °C) because of the fairly low content of isotactic segments. However, we did not want to increase the amount of isotactic PNIPAM, because stereoblock polymers having longer isotactic segments have poor water solubility. The isotactic segments in the stereoblock polymers presented here are of low molar mass, and T_gs of the stereoblock polymers are always lower than that of atactic PNIPAM.

Contrary to expectation, no crystallinity of the isotactic PNIPAM could be observed with DSC in spite of prolonged annealing above T_g. Though the isotacticity of the polymer is fairly high, the finding probably indicates that the amount of irregular atactic sequences is high enough to prevent the crystallization.

3.2.2 Phase separation in bulk

Self-organization leads to nanoscale polymeric structures based on competitive interactions giving rise to hierarchical structures, where primary building blocks organize into more complex secondary structures.[108]

3.2.2.1 *Phase separation of poly(styrene-block-N-isopropylacrylamide)* (unpublished data)

It has been previously demonstrated, how amphiphilic molecules can selectively bond to one block of a block copolymer, leading to structure-within-structures. This concept was used in the preparation of mesoporous materials.[109] In this work, we wanted to go one step further and to introduce functional mesoporosity induced by the PNIPAM block. Several PS-PNIPAM diblock copolymers (data not shown) were complexed with a small organic amphiphile, 4-hexylresorcinol.[110] Polymers organized to expected structures, for example PS_{336}-$PNIPAM_{147}$ formed lamellar-*within*-lamellar structures and PS_{175}-$PNIPAM_{38}$ formed PNIPAM cylinders within PS matrix. Later, the complexed amphiphile was washed away leading to functional pores.

Unfortunately, PNIPAM pores in water did not show any thermoresponse. This is probably due to the simple fact that the PNIPAM layer in the pore was too thick. As a consequence, the PNIPAM "hairs" do not have enough room to collapse upon heating and pores do not open at elevated temperature. Thus, we decided to move to another concept based on A-B-A triblock copolymer gels.

3.2.2.2 Poly(styrene-block-N-isopropylacrylamide-block-styrene) structures in bulk (Paper IV)

One way to exploit the conformational transition of PNIPAM is based on responsive polymer networks in water solutions to form hydrogels and gelators.[111, 112] This concept can be based on ABA triblock copolymers where association can be triggered the by temperature. In the bulk state, triblock copolymers self-assemble into different morphologies.[113] In order to achieve stimuli-responsive hydrogels, the ABA block copolymers can be swollen by solvents selective to the middle block, leading to physically crosslinked gels where the endblock domains form the physical crosslinks.

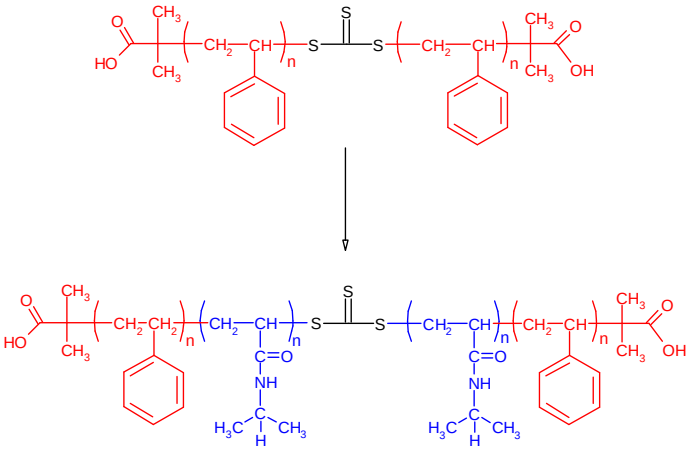

Scheme 8. Poly(styrene-*block*-N-isopropylacrylamide-*block*-styrene)

Here, temperature-responsive PS-PNIPAM-PS triblock copolymers, which may self-assemble in bulk, were synthesized. These polymers were used to prepare aqueous thermo-responsive membranes (Scheme 8). The hydrophobic PS endblocks were selected to form the minority component, whereas PNIPAM midblock accounted for the majority component. The weight fraction of PS was varied and classical lamellar, cylindrical, spherical, and bicontinuous double gyroid morphologies corresponding the phase diagram were observed in the dried state (Table 5 and Figure 7).

***Table 5**. Morphologies of polystyrene-block-poly(N-isopropylacrylamide)-block-polystyrene triblock copolymer. For phase diagram, see IV.*

polymer	M_n (g mol^{-1})	PNIPAM wt%	morphology
PS_{33}-$PNIPAM_{294}$-PS_{33}	40 500	83	spherical
PS_{33}-$PNIPAM_{245}$-PS_{33}	34 900	79	spherical
PS_{131}-$PNIPAM_{805}$-PS_{131}	118 300	77	spherical
PS_{33}-$PNIPAM_{161}$-PS_{33}	25 400	72	spherical
PS_{84}-$PNIPAM_{402}$-PS_{84}	63 200	72	cylindrical
PS_{197}-$PNIPAM_{573}$-PS_{197}	106 000	61	gyroid
PS_{196}-$PNIPAM_{438}$-PS_{196}	90 500	55	lamellar
PS_{176}-$PNIPAM_{244}$-PS_{176}	64 600	43	lamellar

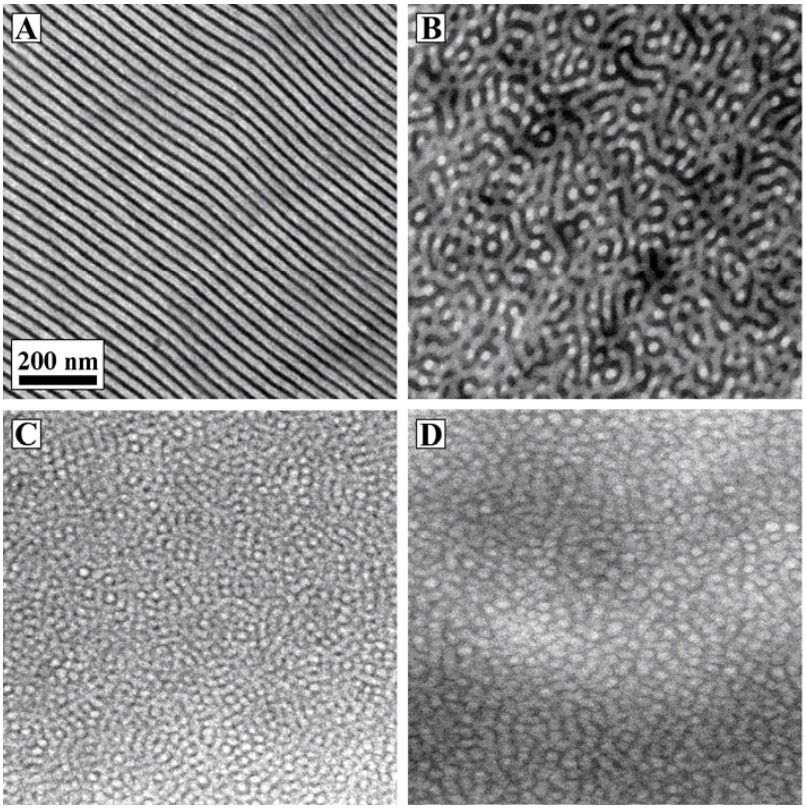

***Figure 7**. Representative TEM micrographs of PS-PNIPAM-PS in bulk: A) PS_{176}-$PNIPAM_{244}$-PS_{176} (43 wt % PNIPAM) is lamellar, B) PS_{197}-$PNIPAM_{573}$-PS_{197} (61 wt % PNIPAM) is gyroid, C) PS_{84}-$PNIPAM_{402}$-PS_{84} (72 wt % PNIPAM) is cylindrical/wormlike, and D) PS_{131}-$PNIPAM_{805}$-PS_{131} is spherical (77 wt % PNIPAM)*

Swelling of hydrogels and hydrogel composite membranes were further studied by Antti Nykänen (Helsinki University of Technology). In summary, the self-assembled bulk morphology plays an important role in the aqueous swelling: PS_{33}-$PNIPAM_{245}$-PS_{33} having spherical self-assembled glassy PS domains in bulk swells below the LCST 58 times of the dry weight. PS_{176}-$PNIPAM_{244}$-PS_{176} with lamellar structure in bulk does not swell in water at any temperature. The gyroid and cylindrical bulk morphologies fall between these extreme cases.

Thin films of PS-PNIPAM-PS were spin coated on top of a macroporous polyacrylonitrile support membrane to form composite membranes. Membranes showed a temperature switchable on/off behavior and efficiently separated low molecular weight species. The results encourage the development of these materials for responsive nanofiltration applications.

3.2.2.3 Organization of gold particles in bulk structures (unpublished data)

Incorporation of nanoparticles into a polymer matrix can have an impact on the material properties. However, the possibilities to control the arrangement of particles are limited. The block copolymers having a rich variety of structures on the nanometer range are one effective way to control particle location and pattern, as nanoparticles can directly self-assemble within block copolymer templates.[114] We demonstrated this concept with PS-PNIPAM-PS triblock copolymers and gold nanoparticles, whose surface was modified to be similar to one of the blocks (PS or PNIPAM). A gold particle/block copolymer composite was dissolved in THF. The solvent was then evaporated from the solution to yield solid sample. In order to obtain thermodynamically stable morphologies the sample was annealed at ca. 180 ºC under a high vacuum. Figure 8 shows a TEM micrograph of PNIPAM-coated gold nanoparticles (see 3.4.1) dispersed in a PS_{176}-$PNIPAM_{244}$-PS_{176} lamellar phase. From the figure it is clear that the particles segregate to the PNIPAM domains (light regions). Likewise, PS protected nanoparticles localized in PS domains. As a conclusion, the arrangement of the nanoparticles was controlled by the surface chemistry.

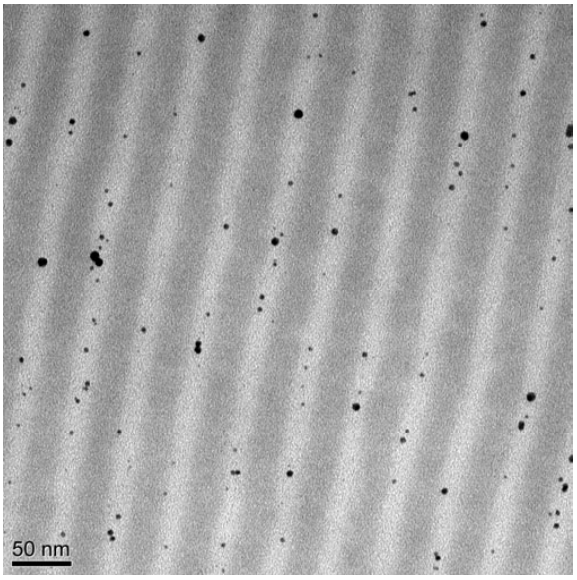

Figure 8. *Cross-sectional TEM images of PNIPAM protected gold nanoparticles incorporated into lamellar PS_{176}-$PNIPAM_{244}$-PS_{176} templates.*

3.3 Aqueous block copolymer dispersions

3.3.1 Studies on the organized polymer structures by light scattering
(Papers II & VI)

The polymers in their aqueous solutions/dispersions were first characterized at room temperature by static and dynamic light scattering. Data obtained from several scattering angles and different concentrations were treated with Zimm double extrapolation which permits the determination of single aggregates properties such as the molar mass of the aggregates ($M_{w,agg}$), aggregation number (N_{agg}), radius of gyration ($<R_g>$) and hydrodynamic radii ($<R_h>$) (Table 6). The average hydrodynamic radii ($<R_h>$) were unimodal and broad, and were not affected by dilution. No angular dependence was found within the experimental error.

Table 6. *Characteristics of diblock and triblock copolymer aggregates measured by light scattering*

Sample	M_n (gmol^{-1})	a-PNIPAM mol%	$<R_g>$ (nm)	$<R_h>$ (nm)	R_g/R_h	$M_{w,agg}$ (10^6 gmol^{-1})	N_{agg}
PS_{48}-$PNIPAM_{346}$	44 300	88	265	300	0.88	167	2813
PS_{75}-$PNIPAM_{118}$	21 400	62	55	38	1.46	10.1	407
$P(t\text{-}BMA)_{135}$-$PNIPAM_{123}$	33 300	47	68	61	1.13	164	164
PNIPAM i2-a28-i2	32 200	89	25	29	0.86	0.82	26
PNIPAM a12-i10-a12	34 300	70	26	21	1.23	0.51	15

a=atactic, i=isotactic PNIPAM sample/block. a-PNIPAM mol% is amount of atactic PNIPAM in block copolymer. Light Scattering measurements were performed at 20 °C, the hydrodynamic radii ($<R_h>$) were measured by DLS. Time correlation functions were analyzed with a Laplace inversion program (Contin). Measurements at several finite angle concentrations by static light scattering were extrapolated in a Zimm plot to determine $<R_g>$, $<R_g>/<R_h>$, M_w of aggregates ($M_{w,agg}$), aggregation number (N_{agg}).

The aggregation process depends on the hydrophobicity of the block copolymers (preparation, see 2.2.1). As is shown in Figure 9, the diameters of the diblock copolymer aggregates vary between 60 and 600 nm at room temperature. Polymer PS_{48}-$PNIPAM_{346}$ forms large aggregates, diameter at room temperature being around 600 nm. The large diameter is due to the long hydrophilic PNIPAM block which disrupts the controlled micelle formation. Two other diblock copolymers polymers PS_{75}-$PNIPAM_{118}$ and $P(t\text{-BMA})_{135}$-$PNIPAM_{123}$ form much smaller structures due to shorter PNIPAM blocks.

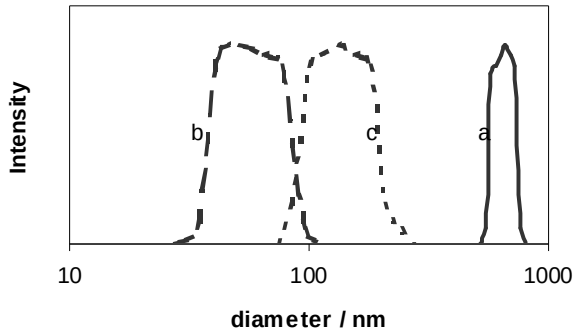

Figure 9. *Size distributions of the aggregates at 20 °C. Polymer concentration 0.2 g/L. a = PS_{48}-$PNIPAM_{346}$, b = PS_{75}-$PNIPAM_{118}$, c = $P(t\text{-}BMA)_{135}$-$PNIPAM_{123}$.*

Values of $\langle R_g \rangle$ / $\langle R_h \rangle$ were examined to get information about the shape of the aggregates.[115] Aggregates of PS_{75}-$PNIPAM_{118}$ and P(*t*-BMA)$_{135}$-$PNIPAM_{123}$ have generally values of $\langle R_g \rangle$ / $\langle R_h \rangle$ greater than 1 indicating a shape of loose spheres. The aggregation number and the radii of these micellar particles are indicative of crew-cut micelles.[116] Structures are visualised in electron micrographs (Figure 10). Crew-cut micelles of PS_{75}-$PNIPAM_{118}$ polymer are separated due to larger PNIPAM content, whereas P(*t*-BMA)$_{135}$-$PNIPAM_{12}$ aggregates can be considered as raspberry like aggregates consisting of several smaller spherical particles.

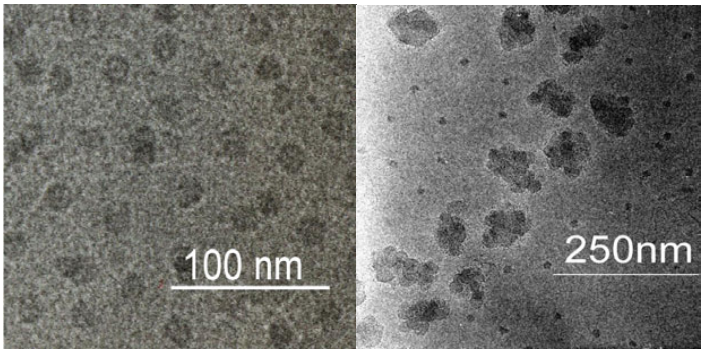

Figure 10. *Cryo-electron microscopy images of aggregate PS_{75}-$PNIPAM_{118}$ (left) and P(t-BMA)$_{135}$-$PNIPAM_{123}$ (right).*

PNIPAM stereoblock polymers are spontaneously water-dispersible. The aggregation number (N_{agg}) and thus, hydrodynamic radii ($<R_h>$) of both studied PNIPAM A-B-A stereoblock polymer aggregates were small (Table 6). However, $<R_h>$ and thus $<R_g>/<R_g>$ reflected a very different conformations of polymers. $<R_g>/<R_h>$ = 0.86 for i2-a28-i2 indicates a uniform spherical structure as a12-i10-a12 having $<R_g>/<R_h>$ = 1.23 can be judged to be a solvent draining structure, coil-like or branched micelle,[115] comparable to crew-cut micelles of diblock copolymers. The densities of the aggregates are much smaller then those predicted for the dense globules indicating that aggregates contain a lot of water inside their hydrodynamic volume.[117, 118] Furthermore, we compared the second virial coefficients (A_2) of the aggregates: $A_2 = 2.2\times10^{-4}$ mol mL/g^2 for i2-a28-i2 and $A_2 = 9.7\times10^{-4}$ mol mL/g^2 for a12-i10-a12. The positive and small values of A_2 indicate that water is a selective solvent for both polymers. The higher A_2 for a12-i10-a12 particles showed that the a12-i10-a12 aggregates are more hydrophilic than i2-a28-i2 aggregates. The result may be aqainst expectations, but this can be well understood with the different block sequences. PNIPAM reach a certain equilibrium aggregate state where water-insoluble isotactic blocks form a core. Water-insoluble block is in a glassy state at ambient temperature stabilizing the formed aggregate structures. i2-a28-i2 forms flower-like particles where short and stiff isotactic end blocks induce the self-organization and associate constructs the inner core, while atactic blocks keep on the periphery forming loops or rings as the corona of the particles. Also, in the case of a12-i10-a12 the isotactic middle block forms the inner core of the micellar aggregates but the atactic blocks are free to stretch out to the solution, this explaining the more hydrophilic structure.

The existence of particles was further evidenced by cryo-TEM (Figure 11, left) and by BF-STEM (Figure 11, right). Most interestingly, flower-like particles of i2-a28-i2 seem to have cavities inside the spherical structures. On the contrary, branched micelles of a12-i10-a12 are visualized as the homogeneous spherical particles. Based on the microscopy images it was further concluded that studied polymers organize very differently in dilute aqueous dispersions depending on their chain.

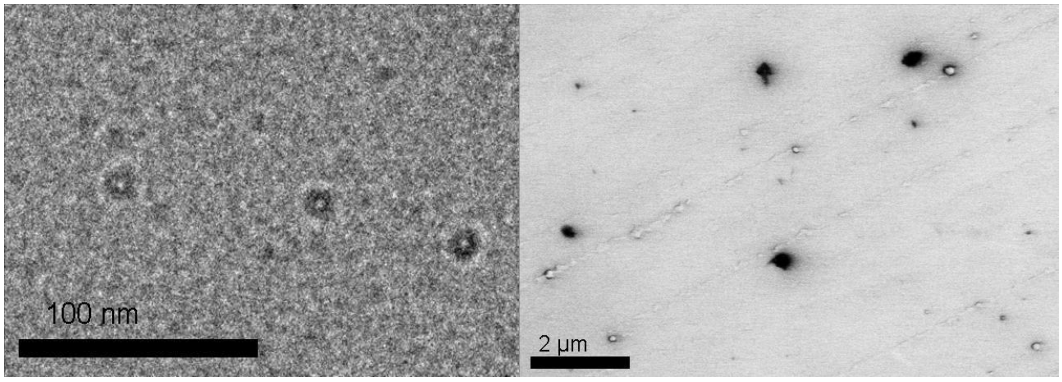

Figure 11. *On the left, Cryo-TEM image of i2-a28-i2 particles in water, c = 3.0 g/L. On the right, BF-STEM image of i2-a28-i2 at room temperature, c = 1.0 g/L.*

The difference between aggregates was observed when they were heated up to 50 ˚C in water. In the case of diblock copolymers, the large aggregates of PS_{48}-$PNIPAM_{346}$ collapsed, and their diameter decreased to 200 nm. Under the same conditions, crew-cut micelles formed by the polymers PS_{75}-$PNIPAM_{118}$ and $P(t\text{-}BMA)_{135}$-$PNIPAM_{123}$ did not shrink considerably upon heating and the aggregation number changed only slightly. It may be assumed that the hydrophobic blocks are long enough to form a dense core and thus, to force PNIPAM to organise as the particle shell. The core-shell structures keep the aggregates stable and reduce the degree of shrinking noticeably when temperature is increased. The surface of the hydrophobic core is crowded in the way that crew-cut micelles are colloidally stable. The precipitation at elevated temperature does not occur even upon prolonged heating at 50 ˚C for several days.

The phase transitions of the A-B-A stereoblock polymer associates were also followed by dynamic light scattering (0.2 g/L, 1.0 g/L and 2.0 g/L). The a12-i10-a12 micelles built up typical intermolecular aggregates above cloud point. This kind of formation of colloidally stable PNIPAM mesoglobules has recently been described in literature.[119] Different self-organization of i2-a28-i2 particles was observed. The $\langle R_h \rangle$ of i2-a28-i2 decreased by ~10 nm when temperature was slowly increased (Figure 12). A moderate decrease means that the the motionally restricted looped chains on the corona of the aggregates compressed. The scattering intensity of the particles is concentration dependent and the demixing temperature is slightly lower at higher concentration (Figure 12). Above 34 °C, a bimodal size distribution of the particles was detected (Figure 13).

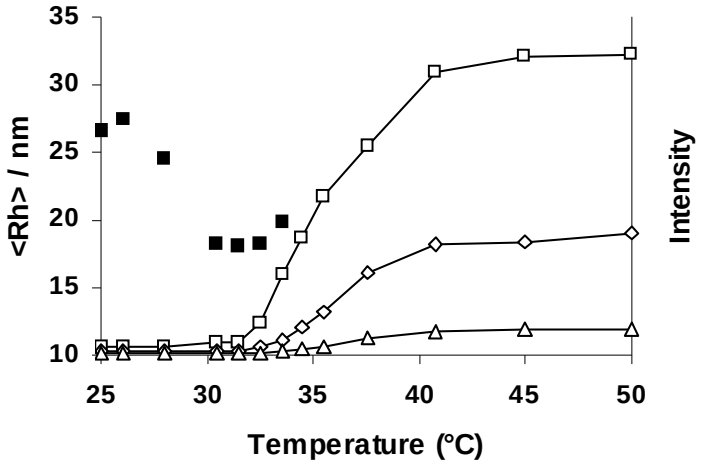

Figure 12*. Hydrodynamic radius of i2-a28-i2, c = 1.0 g/L (■), by dynamic light scattering. Cloud point slightly decreases as concentration increases, c = 0.2 g/L (Δ), c = 1.0 g/L (◊), C = 2.0 g/L (□).*

The bimodal distribution is caused by the partial aggregation of the particles to multimicelle aggregates. A-B-A type amphiphilic polymers with non-water-soluble stickers are known to form flower-like micelles. In addition, amphiphiles may undergo bridging where a network of flowers is connected by bridges.[120, 121] We suppose that in the case of i2-a28-i2 some of the micelles are connected in this way. This kind of system can phase separate into two macrophases, one of them being a phase of collapsed network (large diameter) and the other, a phase of collapsed invididual aggregates (unchanged diameter). Merging of the aggregate particles requires the reformation of the chains in a way similar to re-organization of hydrophobically modified telechelic PNIPAM chains upon heating.[87] Increasing interactions and the dissociation of the intramolecular C=O···H–N hydrogen bonds can force some particles to re-organize and a temperature responsive morphological transition takes place, upon which small particles fuse to bigger ones.[90] Once formed, a12-i10-a12 and i2-a28-i2 mesoglobules are very stable at elevated temperatures even for prolonged time (weeks).

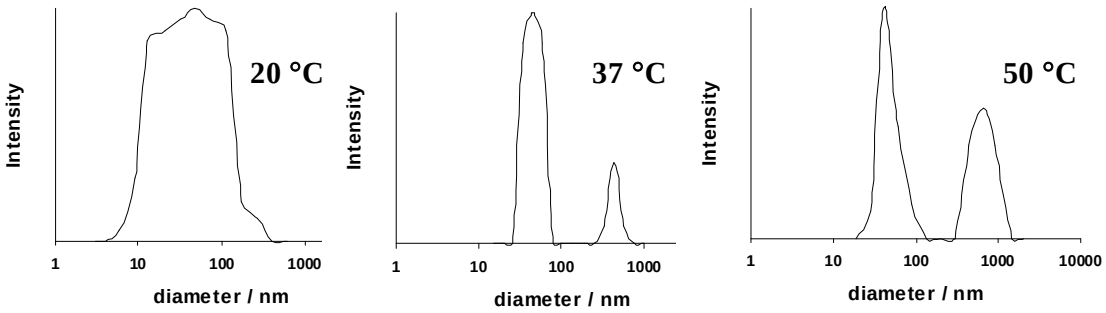

Figure 13*. Size distribution of i2-a28-i2 (c = 1.0 g/L) vesicles and the dependence of hydrodynamic diameter on temperature.*

The temperature induced transitions of the studied particles are completely reversible. The original morphologies were observed again when dispersions were cooled back to ambient temperature. One should also note that even though the thermally induced self-organization at slow heating rates depends on the block sequence, fast-heating protocol provides small mesoglobules typical for linear thermoresponsive polymers.[119]

The high stability upon heating of the i2-a28-i2 particles was also evidenced by turbidity measurements (Figure 14). The transmittance of the stereoblock polymer particles decreased gradually upon heating and transmittance of i2-a28-i2 particles decreased only moderately at elevated temperatures compared to a12-i10-a12 micelles or atactic PNIPAM, which precipitates out from the solution around 35 °C. The observed moderate variation of the transmittance of suspensions of the spherical i2-a28-i2 particles shows that the present sample behaves totally differently from aqueous linear atactic PNIPAM chains.

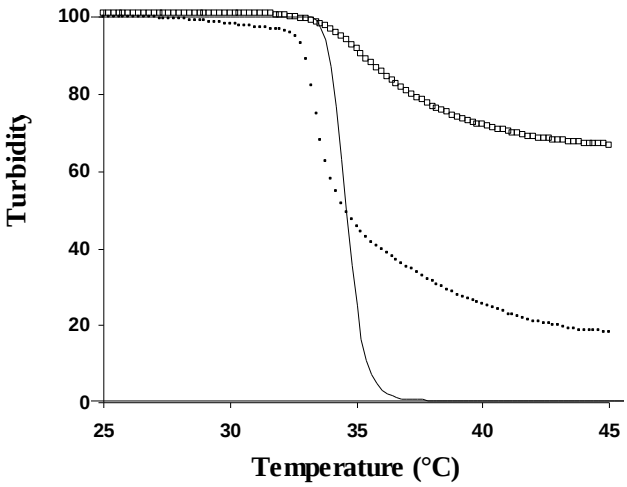

***Figure 14**. Turbidity of aqueous solutions of PNIPAM polymers. i2-a28-i2 (□), a12-i10-a12 (■) and a24.3 (line) measured by UV-vis spectrometry (c = 1.0 g/L, heating rate = 0.2 °Cmin^{-1}).*

3.3.2 **Phase transition measurements of aggregate structures by microcalorimetry** *(Papers II & VI)*

The samples studied by light scattering methods were also analysed by microcalorimetry. Thermograms of the diblock copolymers are shown in Figure 15. The transition of all three diblock copolymer samples had ΔH values within the same range. The phase transition of PS_{48}-$PNIPAM_{346}$, had an onset temperature typical of pure PNIPAM, whereas the more hydrophobic PS_{75}-$PNIPAM_{118}$ and P(*t*-BMA)$_{135}$-$PNIPAM_{123}$ started to dehydrate at noticeably lower temperatures. Thus, hydrophobic blocks lowered the maximum temperature of the dehydration of the PNIPAM brushes. Also, the temperature range of the PNIPAM demixing broadened as the size of the hydrophobe increased in the aggregate core. The dehydration took place over a temperature range ~ 15–40 °C and PNIPAM dehydration is restricted on the stable surface of the crew-cut micelles.

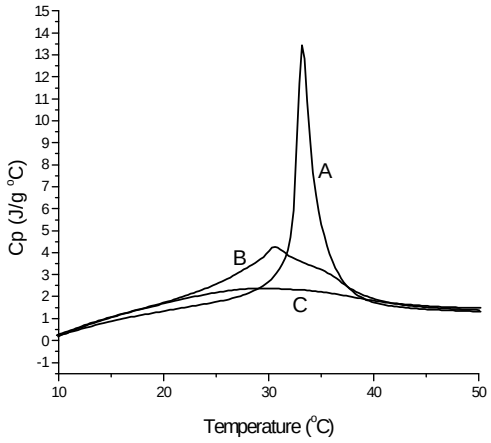

Figure 15. *Thermograms of aqueous solutions, heating rate 1 °C min^{-1}. PNIPAM concentrations in solutions a = PS_{48}-$PNIPAM_{346}$, b = PS_{75}-$PNIPAM_{118}$, c = P(t-BMA)$_{135}$-$PNIPAM_{123}$.: 0.88 g/L, 0.63 g/L and 0.47 g/L.*

Figure 16 shows endotherms of a24.3 homo PNIPAM, i2-a28-i2 and a12-i10-a12 stereoblock copolymers measured by microcalorimetry (c = 1.0 g/L, heating rate = 0.5 °C min^{-1}). The enthalpy of the phase transition (ΔH) per repeating monomer unit for all three samples are 5.9 kJ/mol (a24.3), 5.5 kJ/mol (i2-a28-i2) and 6.0 kJ/mol (a12-i10-a12), corresponding to literature values for PNIPAM, indicating that PNIPAM layer is hydrated below cloud point.[63, 122]. The experiment showed the stereoblock polymers to have broader phase transitions compared to atactic PNIPAM,[118] which is maybe due to the PNIPAM chains locked in a hydrophobic environment on the surface of the particles as in the case of crew-cut micelles. a12-i10-a12 micelles undergo a broad and continuous phase transition. More interestingly, we detected two phase transitions for i2-a28-i2. The first transition is the transition from a random coil to an ordered coil.[123] The second and broader transition corresponds to the intermolecular aggregation of the individual particles and the collapse of the PNIPAM. The collapse temperature of the i2-a28-i2 (35.2 °C) is slightly higher compared to a24.3 PNIPAM (T_m = 34.6 °C). This observation could be rationalized in the following way. Isotactic outer blocks associate

and force stereoblock polymers to form looped, flower-like structures. Higher transition temperature reflects the fact that looped PNIPAM chains on the surface of the locked structures have to overcome an additional internal stress compared to free PNIPAM chains in solution.[123] Further, the water-insoluble blocks function as structure making components increasing the stability of the particles at elevated temperatures.[124]

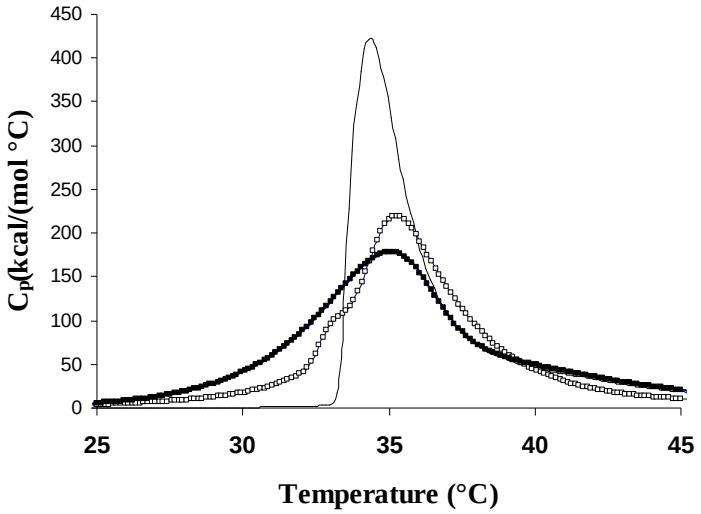

Figure 16. *Microcalorimetric endotherms of aqueous solutions of i2-a28-i2 (□), a12-i10-a12 (■) and a24.3 (line) (c = 1.0 g/L, heating rate = 0.5 °Cmin^{-1}).*

At higher concentrations (90 g/L) studied polymers show only one transition peak, form gels and precipitate above could point temperature.[112] Nojima et al. have also recently studied flower micelles and demonstrated that micellization and gelation, respectively, occur in dilute and concentrated telechelic hydrophobically modified PNIPAM solutions.[125] As enthalpies of the phase transition (ΔH) per repeating unit for all samples are within the same range, it suggests that the structure of the hydration layer around isotactic PNIPAM is similar to that around an atactic chain. It can be assumed that the isotactic chains (which can adopt a helical conformation) form more intramolecular C=O···H–N hydrogen bonds.[56] As a consequence, isotactic sequences reduce the solubility and the flexibility of the polymers. It has been suggested that in addition to the dehydration of the PNIPAM layer, dissociation of intramolecular C=O···H–N hydrogen bonds contributes to the phase transition.[126] We assume that an increased amount of intra- and intermolecular bonds is the reason behind the increased colloidal stability of the stereoblock copolymers, because extra energy is needed to trigger the dissociation of the intramolecular bonds and thus, phase-separation. When concentration is increased, the intermolecular hydrogen bonds increase in number, this eventually leading to gelation.

3.4 Gold Nanoparticles protected with poly(methacrylic acid-*block*-N-isopropylacrylamide)

Block copolymers in selective solvents, where they form micelles, have been used to encapsulate metal particles. The core of the micelle is able to entrap metal salts by complexation or association and the shell of the micelle provides stabilization. These complexes are then reduced or chemically converted to colloidal metal hybrid particles.[20] Polymer protected gold particles can also be synthesized by 'grafting-from' reactions, as we have shown previously.[127]

We have found that polymers bearing a dithioester end group synthesized through the RAFT polymerization can be directly used in the synthesis of polymer grafted nanoparticles. The dithioester end group of PNIPAM was hydrolyzed in the one-pot synthesis to a thiol which immediately protects the forming gold nanoparticles. Next, double stimuli-sensitive PMAA-PNIPAM was also employed to study how the properties of the gold particles can be altered by changing pH and temperature. The dithiobenzoate end group is in the end of the PNIPAM block, and thus, PMAA-NIPAM is expected to bound to the gold surface through the PNIPAM blocks, leaving the PMAA blocks as the outer shell around the particle.

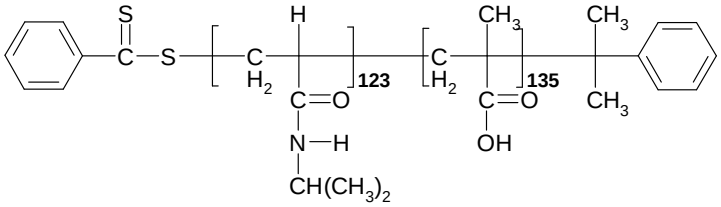

Scheme 9. *Poly(methacrylic acid-block-N-isopropylacrylamide).*

3.4.1 Characterization of polymer protected gold nanoparticles *(Papers I & III)*

The size and size distribution of the gold particles were measured using electron microscopy. The gold core of the particles had reasonably narrow size distributions (Table 7). The total mass loss of the polymer chains bound to the gold cores was determined by TGA. Then, the density of polymer chains was calculated in terms of the surface area of the corresponding gold core divided by the number of polymer chains bound to a surface. The footprint of PNIPAM polymer was estimated to be 0.54 nm^2 / polymer chain corresponding previous reports.[97, 128] Interestingly, the surface area 2.2 nm^2 / polymer chain for PMAA-PNIPAM was higher that for shorter PNIPAM, meaning that the number of polymer chains per gold particle is much lower. On the other hand, the amount of organic material on the surface of the studied gold particles measured by TGA was approximately the same (32 and 29%). Bigger polymers chains ($PMAA_{135}$-$PNIPAM_{123}$) have a larger footprint area on the surface of the gold core and a lower number of polymer chains are needed to protect particles.

Table 7*. Characterization of gold nanoparticles.*

protecting polymer	diameter Au core (nm)	polymer (wt %)	formula of AuNP	footprint nm^2/chain
PNIPAM-5400	2.3 ± 0.8	68	$PNIPAM_{44}Au_{459}$	0.54
$PMAA_{135}$-$PNIPAM_{123}$	2.7 ± 0.4	71	$(PMAA_{135}\text{-}PNIPAM_{123})_{15}Au_{807}$	2.2

Diameter is measured by TEM[128, 129] and the amount of polymer by TGA. footprint = surface area of a gold core / the number of chain bound to the gold core.

3.4.2 **The effect of pH on the gold particles** *(Paper III)*

The colloidal stability of the particles is governed by the PMAA block as they form the outer layer. The solubility of the PMAA block in water depends on the pH of the medium. With lowering the pH the carboxylic groups of the PMAA blocks are protonated and the polymer becomes less soluble in the aqueous medium.

The effect of pH on gold nanoparticles was monitored by optical spectroscopy (Figure 17). The plasmon band of the sample increases as pH decreased as was expected, indicating that the dispersibility of the particles decreased as PMAA was protonated and at pH 4 particles precipitated from water.

When the pH of the solvent is decreased, we simultaneously observe a blue shift in the surface plasmon resonance (SPR) and the λ_{max} shifted around 10 nm to lower wavelengths (Figure 17, inset). The surface plasmon absorption is an optical property for the metallic nanoparticles due to an extensive electronic correlation and corresponds to a collective excitation of conduction electrons relative to the ionic core.[130, 131] The study of the SPR is an area of very active research for its applications in the optical and photographic processes. The SPR band of nanoparticles is also dependent on the dielectric constant of the medium.[132-134]

We have shown previously that the conformational change of the PNIPAM monolayer on the gold nanoparticles at the air-water interface induces a blue-shift.[135] Analogously, we can suggest that in this case the number of water molecules in the proximity of the metal particles decreases with decreasing pH. This is a natural consequence of the decreased solubility of PMAA, especially at pH 5. To summarize, polarity of the particle surroundings decreased with decreasing pH. Thus, optical properties of the nanoparticles can be varied by pH.

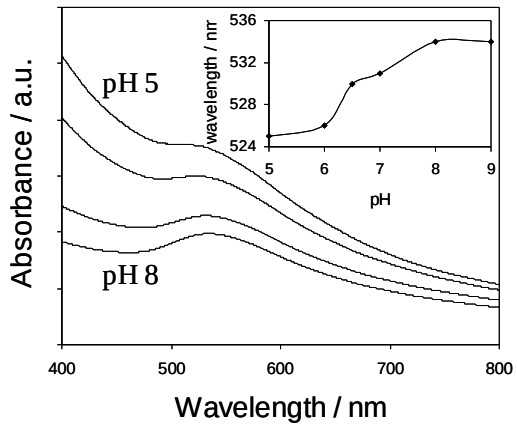

Figure 17. *UV-vis spectra as a function of pH. Turbidity increases as pH is decreased, pH decreases from bottom to top (pH 8, 7, 6, 5). The surface plasmon resonance band undergoes a blue-shift (534 nm to 525 nm) when pH is decreased.*

The hydrodynamic size of the particles was measured by dynamic light scattering. The mean diameter of the scattering objects is around 100 nm at room temperature and pH 7, indicating that the particles form aggregates in water. However, the aggregates are colloidally stable and individual gold cores remain separated (no coupling on SPR). As pH is increased, the dissociated PMAA outer layer stretches the polymers and the size of the aggregate increases slightly. On the other hand, at pH 5 aggregates take more compact structure (d_{mean} = 60nm) than at pH 7.

3.4.3 The effect of temperature on the gold particles *(Paper III)*

The effect of temperature on particles was measured by DLS and UV. When solutions at pH 7 were heated up to 50 °C, the average diameter of the aggregates decreased only slightly, from 102 nm to 88 nm. This indicates that the mobility of the PNIPAM blocks is restricted similarly to the case of crew-cut PS-PNIPAM micelles. At pH 5 the aggregates started to agglomerate and the scattering intensity increased. This effect was observed by turbidity measurements (Figure 18). The macroscopic agglomeration taking place at low pH and elevated temperature was irreversible, which is contrary to the completely reversible phase transition of pure aqueous PNIPAM. Typical phase transition of pure PNIPAM, which takes place over a narrow range of temperatures was not observed even by calorimetry. At neutral or basic conditions the electrically charged PMAA corona shelters the particles keeping them dispersible in water. This stretches the PNIPAM blocks and prevents any conformational changes. At pH 5 the reason for the absence of the PNIPAM thermal transition is different.[136] It has been shown previously by Burova et al.[137] and Diez-Pena et al.[138] that at low pH, hydrogen bonding between PNIPAM and PMAA gives rise to the formation of hydrophobic complexes. Thus, at pH 5, the complexation of two blocks leads to compact aggregates already at room temperature, and PNIPAM at least partially loses its capability to collapse upon heating. This was evidenced by microcalorimetry, where a broad heat capacity peak at low temperatures (maximum at 19 °C) was observed. This corresponds to PNIPAM in a hydrophobic environment as in the case of crew-cut micelles. Also, the transition enthalpy was reduced (1.2 kJ/mol per repeating unit) compared to that of pure PNIPAM. This kind of enthalpy decrease at low pH proves that the partial complexation between PNIPAM and PMAA almost completely suppresses conformational change of the inner PNIPAM core.

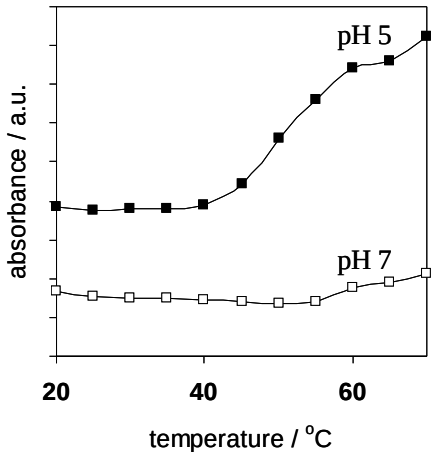

Figure 18. *Turbidity curves of the Au-PNIPAM-PMAA 1.0 g/L in water at two different pH (7.0=□ and 5.0=■).*

Absorption spectra of the dispersions were measured as a function of temperate at pH 5 and 7 to find out if the thermal transition of PNIPAM affects the SPR band even if the macroscopical phase transition of PNIPAM was not observed. As shown in Figure 18, particles at pH 7 remained soluble even at elevated temperature. However, a blue shift as a function of temperature was observed. The shift of λ_{max} to lower wavelengths upon heating (Figure 19) confirmed the occurrence of the conformational change of PNIPAM blocks. Upon heating PNIPAM layer turns hydrophobic squeezing out water molecules from the surroundings of the Au core. This process decreases the dielectric constant of the particle surroundings and blue shift is observed in the SPR. On the other hand, at pH 5 the complexation of PNIPAM and PMAA makes the surroundings of the gold core more hydrophobic and practically no blue shift was detected at low pH upon heating.

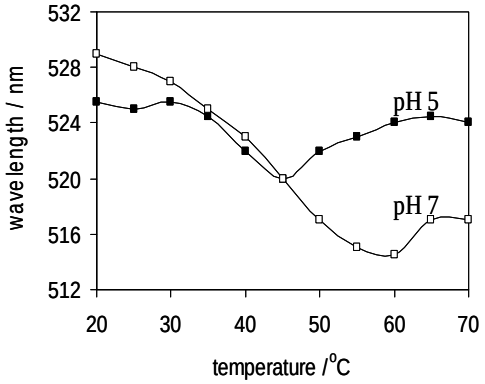

Figure 19. *The λ_{max} of the surface plasmon resonance as a function of temperature at two pH (7.0=□ and 5.0=■).*

As a conclusion, block copolymers make it possible to protect particles in a way that the outer layer colloidally stabilizes the aggregates while the inner layer modulates the polarity of the immediate surroundings of the gold core.

4 CONCLUSIONS

RAFT polymerization and the rapid progress in block copolymer synthesis play a crucial role in sophisticated nanostructured material applications.[7] In this work, a comprehensive understanding of the RAFT polymerization provided a powerful tool for the production of well-designed amphiphilic diblock and triblock copolymers with low polydispersities It was demonstrated, how different pre-designed and precisely synthesized block copolymer materials of PNIPAM organize and form specific structures on the nanoscale, mainly in aqueous solutions.

Multiple block copolymer morphologies in aqueous solutions were demonstrated varying solution conditions and the chemistry of the block copolymers. When dispersed in water, block copolymers form, depending on the chain composition, crew-cut micelles, branched micelle structures or flower-like micelles structure. The block sequence affects strongly the self-organization and thermally induced phase separation. Hydrophobic blocks were observed to influence the stability of the particles. The present work is a new aspect in the fundamental studies considering PNIPAM self-organization and especially stereoregular PNIPAM polymers. The study contributes to the discussion about the effect of chemical composition and stereochemistry on the phase transition of PNIPAM. The findings may be useful to design new thermosensitive, biomimetic structures by stereocontrolled PNIPAM block polymers.

In bulk, the self-assembled morphologies of eight different PS-PNIPAM-PS triblock copolymers were studied, and the phase behavior was investigated using TEM. All the stable block copolymer morphologies were observed, i.e. lamellar, cylindrical, spherical, and gyroidal structures. The self-assembled bulk morphology plays an important role in the aqueous swelling of the hydrogels.

Gold nanoparticles coated with stimuli-responsive PMAA-PNIPAM copolymers were prepared in a convenient one-pot synthesis. It was shown that the association and optical properties of the gold nanoparticles grafted with smart polymers can be widely varied by pH and temperature.

5 REFERENCES

(1) Service, R. F.; Szuromi, P.; Uppenbrink, J. *Science* **2002**, *295*, 2395.

(2) Hamley, I. W. *Angew. Chem. Int. Ed.* **2003**, *42*, 1692-1712.

(3) Lutz, J. F. *Polym. Int.* **2006**, *55*, 979-993.

(4) Ozin, G. A.; Arsenault, A. C. *Nanochemistry*, RSC Publishing, Toronto **2005**, p.585-588.

(5) Vriezema, D. M.; Aragones, M. C.; Elemans, J. A. A. W.; Cornelissen, J. J. L. M.; Rowan, A. E.; Nolte, R. J. M. *Chem. Rev.* **2005**, *105*, 1445-1489.

(6) Mecke, A.; Dittrich, C.; Meier, W. *Soft Matter* **2006**, *2*, 751-759.

(7) Lodge, T. P. *Macromol. Chem. Phys.* **2003**, *204*, 265-273.

(8) Foerster, S.; Antonietti, M. *Adv. Mater.* **1998**, *10*, 195-217.

(9) Riess, G. *Prog. Polym. Sci.* **2003**, *28*, 1107-1170.

(10) Discher, D. E.; Eisenberg, A. *Science* **2002**, *297*, 967-973.

(11) Bates, F. S.; Fredrickson, G. H. *Physics Today* **1999**, *52*, 32-38.

(12) Ikkala, O.; ten Brinke, G. *Chem. Comm.* **2004**, 2131-2137.

(13) Matyjaszewski. K. Davis, T., Eds., *Handbook of Radical Polymerization*, John Wiley & Sons, New York, **2002**.

(14) Braunecker, W. A.; Matyjaszewski, K. *Prog. Polym. Sci.* **2007**, *32*, 93-146.

(15) Pyun, J.; Matyjaszewski, K. *Chem. Mater.* **2001**, *13*, 3436-3448.

(16) Hoffman, A. S.; Stayton, P. S. *Macromol. Symp.* **2004**, *207*, 139-151.

(17) Mertoglu, M.; Garnier, S.; Laschewsky, A.; Skrabania, K.; Storsberg, J. *Polymer* **2005**, *46*, 7726-7740.

(18) Lowe, A. B.; McCormick, C. L. *Prog. Polym. Sci.* **2007**, *32*, 283-351.

(19) Shipway, A. N.; Katz, E.; Willner, I. *ChemPhysChem* **2000**, *1*, 18-52.

(20) Daniel, M.; Astruc, D. *Chem. Rev.* **2004**, *104*, 293-346.

(21) Shan, J. *Chem. Comm.* **2007**, 44, 4580-4598.

(22) Matyjaszewski, K.; Spanswick, J. *Materials Today* **2005**, *8*, 26-33.

(23) Matyjaszewski, K.; Gnanou, Y.; Leibler, L.; Eds. *Macromolecular Engineering*, Volume 4, Wiley-VCH, Weinheim, **2007**.

(24) Szwarc, M. *Nature* **1956**, *178*, 1168-1169.

(25) Szwarc, M. *J. Polym. Sci., Part A: Polym. Chem.* **1998**, *36*, ix-xv.

(26) Webster, O. W. *Science* **1991**, *251*, 887-893.

(27) Hadjichristidis, N.; Pitsikalis, M.; Pispas, S.; Iatrou, H. *Chem. Rev.* **2001**, *101*, 3747-3792.

(28) Percec, V.; Tirrell, D. A. *J. Polym. Sci., Part A: Polym. Chem.* **2000**, *38*, 1705.

(29) Darling, T. R.; Davis, T. P.; Fryd, M.; Gridnev, A. A.; Haddleton, D. M.; Ittel, S. D.; Matheson, R. R., Jr.; Moad, G.; Rizzardo, E. *J. Polym. Sci., Part A: Polym. Chem.* **2000**, *38*, 1706-1708.

(30) Georges, M. K.; Veregin, R. P. N.; Kazmaier, P. M.; Hamer, G. K. *Macromolecules* **1993**, *26*, 2987-2988.

(31) Hawker, C. J.; Bosman, A. W.; Harth, E. *Chem. Rev.* **2001**, *101*, 3661-3688.

(32) Wang, J.; Matyjaszewski, K. *J. Am. Chem. Soc.* **1995**, *117*, 5614-5615.

(33) Chiefari, J.; Chong, Y. K.; Ercole, F.; Krstina, J.; Jeffery, J.; Le, T. P. T.; Mayadunne, R. T. A.; Meijs, G. F.; Moad, C. L.; Moad, G.; Rizzardo, E.; Thang, S. H. *Macromolecules* **1998**, *31*, 5559-5562.

(34) Fischer, H. *Chem. Rev.* **2001**, *101*, 3581-3610.

(35) Solomon, D. H. *J. Polym. Sci., Part A: Polym. Chem.* **2005**, *43*, 5748-5764.

(36) Kato, M.; Kamigaito, M.; Sawamoto, M.; Higashimura, T. *Macromolecules* **1995**, *28*, 1721-1723.

(37) Goto, A.; Fukuda, T. *Prog. Polym. Sci.* **2004**, *29*, 329-385.

(38) Jakubowski, W.; Matyjaszewski, K. *Angew. Chem. Int. Ed.* **2006**, *45*, 4482-4486.

(39) Jakubowski, W.; Min, K.; Matyjaszewski, K. *Macromolecules* **2006**, *39*, 39-45.

(40) Otsu, T.; Yoshida, M. *Makromol. Chem.* **1982**, *3*, 127-132.

(41) Otsu, T. *J. Polym. Sci., Part A: Polym. Chem.* **2000**, *38*, 2121-2136.

(42) Charmot, D.; Corpart, P.; Adam, H.; Zard, S. Z.; Biadatti, T.; Bouhadir, G. *Macromol. Symp.* **2000**, *150*, 23-32.

(43) Perrier, S.; Takolpuckdee, P. *J. Polym. Sci., Part A: Polym. Chem.* **2005**, *43*, 5347-5393.

(44) Moad, G.; Chiefari, J.; Chong, Y. K.; Krstina, J.; Mayadunne, R. T. A.; Postma, A.; Rizzardo, E.; Thang, S. H. *Polym. Int.* **2000**, *49*, 993-1001.

(45) Moad, G.; Rizzardo, E.; Thang, S. H. *Aust. J. Chem.* **2005**, *58*, 379-410.

(46) Mertoglu, M.; Laschewsky, A.; Skrabania, K.; Wieland, C. *Macromolecules* **2005**, *38*, 3601-3614.

(47) Kamigaito, M.; Satoh, K. *Macromolecules* **2008**, *41*, 269-276.

(48) Barner-Kowollik, C.; Buback, M.; Charleux, B.; Coote, M. L.; Drache, M.; Fukuda, T.; Goto, A.; Klumperman, B.; Lowe, A. B.; Mcleary, J. B.; Moad, G.; Monteiro, M. J.; Sanderson, R. D.; Tonge, M. P.; Vana, P. *J. Polym. Sci., Part A: Polym. Chem.* **2006**, *44*, 5809-5831.

(49) Favier, A.; Charreyre, M. *Macromol. Rapid Commun.* **2006**, *27*, 653-692.

(50) Odian, G. *Principles of Polymerization, 4th Ed.*, John Wiley & Sons, New York, **2004**, p.622.

(51) Habaue, S.; Okamoto, Y. *Chem. Rec.* **2001**, *1*, 46-52.

(52) Isobe, Y.; Yamada, K.; Nakano, T.; Okamoto, Y. *Macromolecules* **1999**, *32*, 5979-5981.

(53) Isobe, Y.; Fujioka, D.; Habaue, S.; Okamoto, Y. *J. Am. Chem. Soc.* **2001**, *123*, 7180-7181.

(54) Ray, B.; Isobe, Y.; Morioka, K.; Habaue, S.; Okamoto, Y.; Kamigaito, M.; Sawamoto, M. *Macromolecules* **2003**, *36*, 543-545.

(55) Ray, B.; Isobe, Y.; Matsumoto, K.; Habaue, S.; Okamoto, Y.; Kamigaito, M.; Sawamoto, M. *Macromolecules* **2004**, *37*, 1702-1710.

(56) Ray, B.; Okamoto, Y.; Kamigaito, N.; Sawamoto, M.; Seno, K.; Kanaoka, S.; Aoshima, S. *Polym. J.* **2005**, *37*, 234-237.

(57) Lutz, J.; Neugebauer, D.; Matyjaszewski, K. *J. Am. Chem. Soc.* **2003**, *125*, 6986-6993.

(58) Mori, H.; Sutoh, K.; Endo, T. *Macromolecules* **2005**, *38*, 9055-9065.

(59) Lutz, J.; Kirci, B.; Matyjaszewski, K. *Macromolecules* **2003**, *36*, 3136-3145.

(60) Chong, Y. K.; Moad, G.; Rizzardo, E.; Skidmore, M. A.; Thang, S. H. *Macromolecules* **2007**, *40*, 9262-9271.

(61) Southall, N. T.; Dill, K. A.; Haymet, A. D. J. *J. Phys. Chem. B* **2002**, *106*, 521-533.

(62) Winnik, F. M. *Macromolecules* **1990**, *23*, 233-242.

(63) Schild, H. G. *Prog. Polym. Sci.* **1992**, *17*, 163-249.

(64) Wu, C.; Zhou, S. *Macromolecules* **1995**, *28*, 8381-8387.

(65) Rzaev, Z. M. O.; Dincer, S.; Piskin, E. *Prog. Polym. Sci.* **2007**, *32*, 534-595.

(66) Chen, G.; Hoffman, A. S. *Nature* **1995**, *373*, 49-52.

(67) Arotcarena, M.; Heise, B.; Ishaya, S.; Laschewsky, A. *J. Am. Chem. Soc.* **2002**, *124*, 3787-3793.

(68) Schilli, C. M.; Zhang, M.; Rizzardo, E.; Thang, S. H.; Chong, Y. K.; Edwards, K.; Karlsson, G.; Mueller, A. H. E. *Macromolecules* **2004**, *37*, 7861-7866.

(69) Skrabania, K.; Kristen, J.; Laschewsky, A.; Akdemir, O.; Hoth, A.; Lutz, J. *Langmuir* **2007**, *23*, 84-93.

(70) Eliassaf, J.; Silberberg, A. *Polymer* **1962**, *3*, 555-564.

(71) Olea, A. F.; Thomas, J. K. *Macromolecules* **1989**, *22*, 1165-1169.

(72) Bates, F. S.; Fredrickson, G. H. *Annu. Rev. Phys. Chem.* **1990**, *41*, 525-557.

(73) Muthukumar, M.; Ober, C. K.; Thomas, E. L. *Science* **1997**, *277*, 1225-1232.

(74) Hamley, I. W. *Introduction to Soft Matter*, John Wiley & Sons, New York, **2007**.

(75) Antonietti, M.; Foerster, S. *Adv. Mater.* **2003**, *15*, 1323-1333.

(76) Zhang, L.; Eisenberg, A. *Science* **1995**, *268*, 1728-1731.

(77) Jain, S.; Bates, F. S. *Science* **2003**, *300*, 460-464.

(78) Hamley, I. W. *Soft Matter* **2005**, *1*, 36-43.

(79) Zhou, J.; Wang, L.; Yang, Q.; Liu, Q.; Yu, H.; Zhao, Z. *J. Phys. Chem. B* **2007**, *111*, 5573-5580.

(80) Pochan, D. J.; Chen, Z.; Cui, H.; Hales, K.; Qi, K.; Wooley, K. L. *Science* **2004**, *306*, 94-97.

(81) Grumelard, J.; Taubert, A.; Meier, W. *Chem. Comm.* **2004**, 1462-1463.

(82) Nardin, C.; Hirt, T.; Leukel, J.; Meier, W. *Langmuir* **2000**, *16*, 1035-1041.

(83) Zhou, X.; Ye, X.; Zhang, G. *J. Phys. Chem. B* **2007**, *111*, 5111-5115.

(84) Reynhout, I. C.; Cornelissen, J. J. L. M.; Nolte, R. J. M. *J. Am. Chem. Soc.* **2007**, *129*, 2327-2332.

(85) Brannan, A. K.; Bates, F. S. *Macromolecules* **2004**, *37*, 8816-8819.

(86) Zhou, Y.; Jiang, K.; Song, Q.; Liu, S. *Langmuir* **2007**, *23*, 13076-13084.

(87) Kujawa, P.; Tanaka, F.; Winnik, F. M. *Macromolecules* **2006**, *39*, 3048-3055.

(88) Cui, H.; Chen, Z.; Zhong, S.; Wooley, K. L.; Pochan, D. J. *Science* **2007**, *317*, 647-650.

(89) LaRue, I.; Adam, M.; Pitsikalis, M.; Hadjichristidis, N.; Rubinstein, M.; Sheiko, S. S. *Macromolecules* **2006**, *39*, 309-314.

(90) Zhou, Y.; Yan, D.; Dong, W.; Tian, Y. *J. Phys. Chem. B* **2007**, *111*, 1262-1270.

(91) Katz, E.; Willner, I. *Angew. Chem. Int. Ed.* **2004**, *43*, 6042-6108.

(92) Templeton, A. C.; Wuelfing, W. P.; Murray, R. W. *Acc. Chem. Res.* **2000**, *33*, 27-36.

(93) Corti, C. W.; Holliday, R. J. *Gold Bull.* **2004**, *37*, 20-26.

(94) Brust, M.; Walker, M.; Bethell, D.; Schiffrin, D. J.; Whyman, R. *Chem. Comm.* **1994**, 801-802.

(95) Storhoff, J. J.; Elghanian, R.; Mucic, R. C.; Mirkin, C. A.; Letsinger, R. L. *J. Am. Chem. Soc.* **1998**, *120*, 1959-1964.

(96) Teranishi, T.; Kiyokawa, I.; Miyake, M. *Adv. Mater.* **1998**, *10*, 596-599.

(97) Wuelfing, W. P.; Gross, S. M.; Miles, D. T.; Murray, R. W. *J. Am. Chem. Soc.* **1 1998**, *120*, 12696-12697.

(98) Corbierre, M. K.; Cameron, N. S.; Sutton, M.; Mochrie, S. G. J.; Lurio, L. B.; Ruehm, A.; Lennox, R. B. *J. Am. Chem. Soc.* **2001**, *123*, 10411-10412.

(99) Corbierre, M. K.; Cameron, N. S.; Lennox, R. B. *Langmuir* **2004**, *20*, 2867-2873.

(100) Lowe, A. B.; Sumerlin, B. S.; Donovan, M. S.; McCormick, C. L. *J. Am. Chem. Soc.* **2002**, *124*, 11562-11563.

(101) Thang, S. H.; Chong, Y. K.; Mayadunne, R. T. A.; Moad, G.; Rizzardo, E. *Tetrahedron Lett.* **1999**, *40*, 2435-2438.

(102) Lai, J. T.; Filla, D.; Shea, R. *Macromolecules* **2002**, *35*, 6754-6756.

(103) Ganachaud, F.; Monteiro, M. J.; Gilbert, R. G.; Dourges, M.; Thang, S. H.; Rizzardo, E. *Macromolecules* **2000**, *33*, 6738-6745.

(104) Mitsukami, Y.; Donovan, M. S.; Lowe, A. B.; McCormick, C. L. *Macromolecules* **2001**, *34*, 2248-2256.

(105) Schilli, C.; Lanzendoerfer, M. G.; Mueller, A. H. E. *Macromolecules* **2002**, *35*, 6819-6827.

(106) Rizzardo, E.; Chen, M.; Chong, B.; Moad, G.; Skidmore, M.; Thang, S. H. *Macromol. Symp.* **2007**, *248*, 104-116.

(107) Ito, M.; Ishizone, T. *J. Polym. Sci., Part A: Polym. Chem.* **2006**, *44*, 4832-4845.

(108) Ikkala, O.; ten Brinke, G. *Science* **2002**, *295*, 2407-2409.

(109) Maki-Ontto, R.; de Moel, K.; de Odorico, W.; Ruokolainen, J.; Stamm, M.; ten Brinke, G.; Ikkala, O. *Adv. Mater.* **2001**, *13*, 117-121.

(110) Ikkala, O. *in Polymeerit tulevaisuuden rakentajina*; Teknologia ohjelmaraportti, TEKES, Sipoo, **2004**, p.56-57.

(111) Li, C.; Tang, Y.; Armes, S. P.; Morris, C. J.; Rose, S. F.; Lloyd, A. W.; Lewis, A. L. *Biomacromolecules* **2005**, *6*, 994-999.

(112) Hietala, S.; Nuopponen, M.; Kalliomäki, K.; Tenhu, H. *Macromolecules* **2008,** 41, 2627-2631.

(113) Matsen, M. W.; Thompson, R. B. *J. Chem. Phys.* **1999**, *111*, 7139-7146.

(114) Lopes, W. A.; Jaeger, H. M. *Nature* **2001**, *414*, 735-738.

(115) Burchard, W. *in Light Scattering Principles and Development*; Brown, W., Ed.; Claredon Press Oxford, **1996**, p 439.

(116) Förster, S.; Zisenis, M.; Wenz, E.; Antonietti, M. *J. Chem. Phys.* **1996**, *104*, 9956-9970.

(117) Marchetti, M.; Prager, S.; Cussler, E. L. *Macromolecules* **1990**, *23*, 3445-3450.

(118) Wu, C.; Wang, X. *Phys. Rev. Lett.* **1998**, *80*, 4092-4094.

(119) Aseyev, V. O.; Tenhu, H.; Winnik, F. M. *Adv. Polym. Sci.* **2006**, *196*, 1-85.

(120) Semenov, A. N.; Joanny, J.; Khokhlov, A. R. *Macromolecules* **1995**, *28*, 1066-1075.

(121) Borisov, O. V.; Halperin, A. *Macromolecules* **1996**, *29*, 2612-2617.

(122) Shan, J.; Chen, J.; Nuopponen, M.; Tenhu, H. *Langmuir* **2004**, *20*, 4671-4676.

(123) Zhang, G.; Winnik, F. M.; Wu, C. *Phys. Rev. Lett.* **2003**, *90*, 035506/1-035506/4.

(124) Zhang, G. Z.; Wu, C. *Adv. Polym. Sci.* **2006**, *195*, 101-176.

(125) Nojima, R.; Sato, T.; Qiu, X.; Winnik, F. M. *Macromolecules* **2008**, *41*, 292-294.

(126) Katsumoto, Y.; Tanaka, T.; Ihara, K.; Koyama, M.; Ozaki, Y. *J. Phys. Chem. B* **2007**, *111*, 12730-12737.

(127) Raula, J.; Shan, J.; Nuopponen, M.; Niskanen, A.; Jiang, H.; Kauppinen, E. I.; Tenhu, H. *Langmuir* **2003**, *19*, 3499-3504.

(128) Hostetler, M. J.; Wingate, J. E.; Zhong, C.; Harris, J. E.; Vachet, R. W.; Clark, M. R.; Londono, J. D.; Green, S. J.; Stokes, J. J.; Wignall, G. D.; Glish, G. L.; Porter, M. D.; Evans, N. D.; Murray, R. W. *Langmuir* **1998**, *14*, 17-30.

(129) Whetten, R. L.; Khoury, J. T.; Alvarez, M. M.; Murthy, S.; Vezmar, I.; Wang, Z. L.; Stephens, P. W.; Cleveland, C. L.; Luedtke, W. D.; Landman, U. *Adv. Mater.* **1996**, *8*, 428-433.

(130) Kreibig, U.; Vollmer, M., Eds. *Optical Properties of Metal Klusters;* Springer Series in Material Science 25; Springer-Verlag, Berlin, **1995**.

(131) Liz-Marzan, L. M. *Langmuir* **2006**, *22*, 32-41.

(132) Mulvaney, P. *Langmuir* **1996**, *12*, 788-800.

(133) Templeton, A. C.; Pietron, J. J.; Murray, R. W.; Mulvaney, P. *J. Phys. Chem. B* **2000**, *104*, 564-570.

(134) Ghosh, S. K.; Nath, S.; Kundu, S.; Esumi, K.; Pal, T. *J. Phys. Chem. B* **2004**, *108*, 13963-13971.

(135) Shan, J.; Chen, J.; Nuopponen, M.; Viitala, T.; Jiang, H.; Peltonen, J.; Kauppinen, E.; Tenhu, H. *Langmuir* **2006**, *22*, 794-801.

(136) Zhang, J.; Peppas, N. A. *Macromolecules* **2000**, *33*, 102-107.

(137) Burova, T. V.; Grinberg, N. V.; Grinberg, V. Y.; Kalinina, E. V.; Lozinsky, V. I.; Aseyev, V. O.; Holappa, S.; Tenhu, H.; Khokhlov, A. R. *Macromolecules* **2005**, *38*, 1292-1299.

(138) Diez-Pena, E.; Quijada-Garrido, I.; Barrales-Rienda, J. M.; Schnell, I.; Spiess, H. W. *Macromol. Chem. Phys.* **2004**, *205*, 438-447.